PCT WORLD INTELLECTUAL PROPERTY ORGANIZATION
International Bureau

INTERNATIONAL APPLICATION PUBLISHED UNDER THE PATENT COOPERATION TREATY (PCT)

(51) International Patent Classification 6 : G06K 9/00, G01N 15/14 — A1

(11) International Publication Number: **WO 97/43732**

(43) International Publication Date: 20 November 1997 (20.11.97)

(21) International Application Number: PCT/CA97/00301

(22) International Filing Date: 1 May 1997 (01.05.97)

(30) Priority Data:
08/644,893 10 May 1996 (10.05.96) US

(71) Applicant: ONCOMETRICS IMAGING CORP. [CA/CA]; 505 - 601 West Broadway, Vancouver, British Columbia V5Z 4C2 (CA).

(72) Inventors: MacAULAY, Calum, E.; 5791 Prince Albert Street, Vancouver, British Columbia V5W 3E1 (CA). PALCIC, Branko; 5357 Trafalgar Street, Vancouver, British Columbia V6N 1B8 (CA). GARNER, David, M.; 838 West 69th Avenue, Vancouver, British Columbia V6P 2W5 (CA). HARRISON, S., Alan; 3884 West 29th Avenue, Vancouver, British Columbia V6S 1T8 (CA).

(74) Agents: REGEHR, Herbert, B. et al.; Bull, Housser & Tupper, 3000 Royal Centre, P.O. Box 11130, 1055 West Georgia Street, Vancouver, British Columbia V6E 3R3 (CA).

(81) Designated States: AL, AM, AT, AU, AZ, BA, BB, BG, BR, BY, CA, CH, CN, CU, CZ, DE, DK, EE, ES, FI, GB, GE, GH, HU, IL, IS, JP, KE, KG, KP, KR, KZ, LC, LK, LR, LS, LT, LU, LV, MD, MG, MK, MN, MW, MX, NO, NZ, PL, PT, RO, RU, SD, SE, SG, SI, SK, TJ, TM, TR, TT, UA, UG, UZ, VN, YU, ARIPO patent (GH, KE, LS, MW, SD, SZ, UG), Eurasian patent (AM, AZ, BY, KG, KZ, MD, RU, TJ, TM), European patent (AT, BE, CH, DE, DK, ES, FI, FR, GB, GR, IE, IT, LU, MC, NL, PT, SE), OAPI patent (BF, BJ, CF, CG, CI, CM, GA, GN, ML, MR, NE, SN, TD, TG).

Published
With international search report.

(54) Title: METHOD AND APPARATUS FOR AUTOMATICALLY DETECTING MALIGNANCY-ASSOCIATED CHANGES

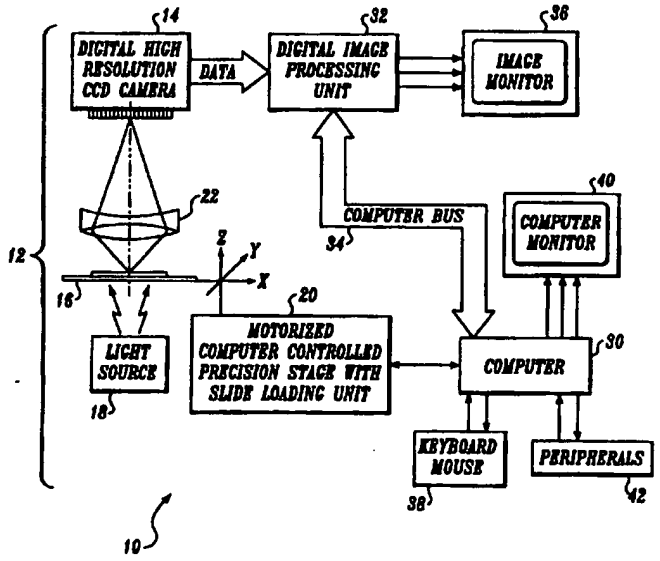

(57) Abstract

A method for detecting malignancy-associated changes. A sample of cells is obtained and stained to identify the nuclear DNA material. The sample is imaged with a digital microscope. Objects of interest are identified in the sample of cells based on the intensity of the pixels that comprise the object versus the average intensity of all pixels in the slide image. An exact edge is located for each object and variations in the illumination intensity of the microscope are compensated for. A computer system calculates feature values for each object and, based on the value of the features, a determination is made whether the cell exhibits malignancy-associated changes or not.

FOR THE PURPOSES OF INFORMATION ONLY

Codes used to identify States party to the PCT on the front pages of pamphlets publishing international applications under the PCT.

AL	Albania
AM	Armenia
AT	Austria
AU	Australia
AZ	Azerbaijan
BA	Bosnia and Herzegovina
BB	Barbados
BE	Belgium
BF	Burkina Faso
BG	Bulgaria
BJ	Benin
BR	Brazil
BY	Belarus
CA	Canada
CF	Central African Republic
CG	Congo
CH	Switzerland
CI	Côte d'Ivoire
CM	Cameroon
CN	China
CU	Cuba
CZ	Czech Republic
DE	Germany
DK	Denmark
EE	Estonia
ES	Spain
FI	Finland
FR	France
GA	Gabon
GB	United Kingdom
GE	Georgia
GH	Ghana
GN	Guinea
GR	Greece
HU	Hungary
IE	Ireland
IL	Israel
IS	Iceland
IT	Italy
JP	Japan
KE	Kenya
KG	Kyrgyzstan
KP	Democratic People's Republic of Korea
KR	Republic of Korea
KZ	Kazakstan
LC	Saint Lucia
LI	Liechtenstein
LK	Sri Lanka
LR	Liberia
LS	Lesotho
LT	Lithuania
LU	Luxembourg
LV	Latvia
MC	Monaco
MD	Republic of Moldova
MG	Madagascar
MK	The former Yugoslav Republic of Macedonia
ML	Mali
MN	Mongolia
MR	Mauritania
MW	Malawi
MX	Mexico
NE	Niger
NL	Netherlands
NO	Norway
NZ	New Zealand
PL	Poland
PT	Portugal
RO	Romania
RU	Russian Federation
SD	Sudan
SE	Sweden
SG	Singapore
SI	Slovenia
SK	Slovakia
SN	Senegal
SZ	Swaziland
TD	Chad
TG	Togo
TJ	Tajikistan
TM	Turkmenistan
TR	Turkey
TT	Trinidad and Tobago
UA	Ukraine
UG	Uganda
US	United States of America
UZ	Uzbekistan
VN	Viet Nam
YU	Yugoslavia
ZW	Zimbabwe

METHOD AND APPARATUS FOR AUTOMATICALLY DETECTING MALIGNANCY-ASSOCIATED CHANGES

Related Applications

The present application is a continuation-in-part of our previous application Serial No. 08/425,257 filed April 17, 1995, which was a continuation of 08/182,453 filed January 10, 1994, which was a continuation-in-part of 07/961,596 filed October 14, 1992, the disclosures of which are incorporated by reference. The benefit of the filing dates of the previous applications are claimed under 35 U.S.C. § 120.

Field of the Invention

The present invention relates to image cytometry systems in general, and in particular to automated systems for detecting malignancy-associated changes in cell nuclei.

Background of the Invention

The most common method of diagnosing cancer in patients is by obtaining a sample of the suspect tissue and examining it under a microscope for the presence of obviously malignant cells. While this process is relatively easy when the location of the suspect tissue is known, it is not so easy when there is no readily identifiable tumor or pre-cancerous lesion. For example, to detect the presence of lung cancer from a sputum sample requires one or more relatively rare cancer cells to be present in the sample. Therefore patients having lung cancer may not be diagnosed properly if the sample does not accurately reflect the conditions of the lung.

Malignancy-associated changes (MACs) are subtle changes that are known to take place in the nuclei of apparently normal cells found near cancer tissue. In addition, MACs have been detected in tissue found near pre-cancerous lesions.

Because the cells exhibiting MACs are more numerous than the malignant cells, MACs offer an additional way of diagnosing the presence of cancer, especially in cases where no cancerous cells can be located.

Despite the ability of researchers to detect MACs in patients known to have cancer or a pre-cancerous condition, MACs have not yet achieved wide acceptance as a screening tool to determine whether a patient has or will develop cancer. Traditionally, MACs have been detected by carefully selecting a cell sample from a location near a tumor or pre-cancerous lesion and viewing the cells under relatively high magnification. However, it is believed that the malignancy-associated changes that take place in the cells are too subtle to be reliably detected by a human pathologist working with conventional microscopic equipment, especially when the pathologist does not know beforehand if the patient has cancer or not. For example, a malignancy-associated change may be indicated by the distribution of DNA within the nucleus coupled with slight variations in the shape of the nucleus edge. However, nuclei from normal cells may exhibit similar types of changes but not to the degree that would signify a MAC. Because human operators cannot easily quantify such subtle cell changes, it is difficult to determine which cells exhibit MACs. Furthermore, the changes which indicate a MAC may vary between different types of cancer, thereby increasing the difficulty of detecting them.

Summary of the Invention

The present invention is a system for automatically detecting malignancy-associated changes in cell samples. The system includes a digital microscope having a CCD camera that is controlled by and interfaced with a computer system. Images captured by the digital microscope are stored in an image processing board and manipulated by the computer system to detect the presence of malignancy-associated changes (MACs). At the present state of the art, it is believed that any detection of MACs requires images to be captured at a high spatial resolution, a high photometric resolution, that all information coming from the nucleus is in focus, that all information belongs to the nucleus (rather than some background), and that there is an accurate and reproducible segmentation of the nucleus and nuclear material. Each of these steps is described in detail below.

To detect the malignancy-associated changes, a cell sample is obtained and stained to identify the nuclear material of the cells and is imaged by the microscope. The stain is stoichiometric and specific to DNA only. The computer system then analyzes the image to compute a histogram of all pixels comprising the image. First, an intensity threshold is set that divides the background pixels from those comprising

the objects in the image. All pixels having an intensity value less than the threshold are identified as possible objects of interest while those having an intensity value greater than the threshold are identified as background and are ignored.

For each object located, the computer system calculates the area, shape and optical density of the object. Those objects that could not possibly be cell nuclei are ignored. Next, the image is decalibrated, i.e., corrected by subtracting an empty frame captured before the scanning of the slide from the current frame and adding back an offset value equal to the average background light level. This process corrects for any shading of the system, uneven illumination, and other imperfections of the image acquisition system. Following decalibration, the images of all remaining objects must be captured in a more precise focus. This is achieved by moving the microscope in the stage z-direction in multiple focal planes around the approximate frame focus. For each surviving object a contrast function (a texture feature) is calculated. The contrast function has a peak value at the exact focus of the object. Only the image at the highest contrast value is retained in the computer memory and any object which did not reach such a peak value is also discarded from further considerations.

Each remaining in-focus object on the image is further compensated for local absorbency of the materials surrounding the object. This is a local decalibration which is similar to that described for the frame decalibration described above, except that only a small subset of pixels having an area equal to the area of a square into which the object will fit is corrected using an equivalent square of the empty frame.

After all images are corrected with the local decalibration procedure, the edge of the object is calculated, i.e., the boundary which determines which pixels in the square belong to the object and which belong to the background. The edge determination is achieved by the edge-relocation algorithm. In this process, the edge of the original mask of the first contoured frame of each surviving object is dilated for several pixels inward and outward. For every pixel in this frame a gradient value is calculated, i.e., the sum and difference between all neighbor pixels touching the pixel in question. Then the lowest gradient value pixel is removed from the rim, subject to the condition that the rim is not ruptured. The process continues until such time as a single pixel rim remains. To ensure that the proper edge of an object is located, this edge may be again dilated as before, and the process repeated until such time as the new edge is identical to the previous edge. In this way the edge is calculated along the highest local gradient.

The computer system then calculates a set of feature values for each object. For some feature calculations the edge along the highest gradient value is corrected by either dilating the edge by one or more pixels or eroding the edge by one or more pixels. This is done such that each feature achieves a greater discriminating power between classes of objects and is thus object specific. These feature values are then analyzed by a classifier that uses the feature values to determine whether the object is an artifact or is a cell nucleus. If the object appears to be a cell nucleus, then the feature values are further analyzed by the classifier to determine whether the nucleus exhibits malignancy-associated changes. Based on the number of objects found in the sample that appear to have malignancy-associated changes and/or an overall malignancy-associated score, a determination can be made whether the patient from whom the cell sample was obtained is healthy or harbors a malignant growth.

Brief Description of the Drawings

The foregoing aspects and many of the attendant advantages of this invention will become more readily appreciated as the same becomes better understood by reference to the following detailed description, when taken in conjunction with the accompanying drawings, wherein:

FIGURE 1 is a block diagram of the MAC detection system according to the present invention;

FIGURES 2A-2C are a series of flow charts showing the steps performed by the present invention to detect MACs;

FIGURE 3 is an illustrative example of a histogram used to separate objects of interest from the background of a slide;

FIGURE 4 is a flow chart of the preferred staining procedure used to prepare a cell sample for the detection of MACs;

FIGURES 5 and 6 are illustrations of objects located in an image;

FIGURES 7A-7F illustrate how the present invention operates to locate the edge of an object;

FIGURES 8 and 9 are diagrammatic illustrations of a classifier that separates artifacts from cell nuclei and MAC nuclei from non-MAC nuclei; and

FIGURE 10 is a flow chart of the steps performed by the present invention to determine whether a patient is normal or abnormal based on the presence of MACs.

Detailed Description of the Preferred Embodiment

As described above, the present invention is a system for automatically detecting malignancy-associated changes (MACs) in the nuclei of cells obtained from

a patient. From the presence or absence of MACs, a determination can be made whether the patient has a malignant cancer.

A block diagram of the MAC detection system according to the present invention is shown in FIGURE 1. The system 10 includes a digital microscope 12 that is controlled by and interfaced with a computer system 30. The microscope 12 preferably has a digital CCD camera 14 employing a scientific CCD having square pixels of approximately 0.3 μm by 0.3 μm size. The scientific CCD has a 100% fill factor and at least a 256 gray level resolution. The CCD camera is preferably mounted in the primary image plane of a planar objective lens 22 of the microscope 12.

A cell sample is placed on a motorized stage 20 of the microscope whose position is controlled by the computer system 30. The motorized stage preferably has an automatic slide loader so that the process of analyzing slides can be completely automated.

A stable light source 18, preferably with feedback control, illuminates the cell sample while an image of the slide is being captured by the CCD camera. The lens 22 placed between the sample 16 and the CCD camera 14 is preferably a 20x/0.75 objective that provides a depth of field in the range of 1-2 μm that yields a distortion-free image. In the present embodiment of the invention, the digital CCD camera 14 used is the Microimager™ produced by Xillix Technologies Corp. of Richmond, B.C., Canada.

The images produced by the CCD camera are received by an image processing board 32 that serves as the interface between the digital camera 14 and the computer system 30. The digital images are stored in the image processing board and manipulated to facilitate the detection of MACs. The image processing board creates a set of analog video signals from the digital image and feeds the video signals to an image monitor 36 in order to display an image of the objects viewed by the microscope.

The computer system 30 also includes one or more input devices 38, such as a keyboard and mouse, as well as one or more peripherals 42, such as a mass digital storage device, a modem or a network card for communicating with a remotely located computer, and a monitor 40.

FIGURES 2A-2C show the steps performed by the system of the present invention to determine whether a sample exhibits MACs or not. Beginning with a step 50, a cell sample is obtained. Cells may be obtained by any number of conventional methods such as biopsy, scraping, etc. The cells are affixed to a slide

and stained using a modified Feulgen procedure at a step 52 that identifies the nuclear DNA in the sample. The details of the staining procedure are shown in FIGURE 4 and described in detail below.

At step 54, an image of a frame from the slide is captured by the CCD camera and is transferred into the image processor. In this process, the CCD sensor within the camera is cleared and a shutter of the camera is opened for a fixed period that is dependent on the intensity of the light source 18. After the image is optimized according to the steps described below, the stage then moves to a new position on the slide such that another image of the new frame can be captured by the camera and transferred into the computer memory. Because the cell sample on the slide occupies a much greater area than the area viewed by the microscope, a number of slide images are used to determine whether the sample is MAC-positive or negative. The position of each captured image on the slide is recorded in the computer system so that the objects of interest in the image can be found on the slide if desired.

Once an image from the slide is captured by the CCD camera and stored in the image processing board, the computer system determines whether the image produced by the CCD camera is devoid of objects. This is performed by scanning the digital image for dark pixels. If the number of dark pixels, i.e., those pixels having an intensity of the background intensity minus a predetermined offset value, is fewer than a predetermined minimum, the computer system assumes that the image is blank and the microscope stage is moved to a new position at step 60 and a new image is captured at step 54.

If the image is not blank, then the computer system attempts to globally focus the image. In general, when the image is in focus, the objects of interest in the image have a maximum darkness. Therefore, for focus determination the height of the stage is adjusted and a new image is captured. The darkness of the object pixels is determined and the process repeats until the average darkness of the pixels in the image is a maximum. At this point, the computer system assumes that global focus has been obtained.

After performing the rough, global focus at step 62, the computer system computes a histogram of all pixels. As shown in FIGURE 3, a histogram is a plot of the number of pixels at each intensity level. In the Microimager™-based microscope system, each pixel can have an intensity ranging from 0 (maximum darkness) to 255 (maximum brightness). The histogram typically contains a first peak 90 that represents the average intensity of the background pixels. A second, smaller peak 92 represents the average intensity of the pixels that comprise the objects. By calculating

a threshold 94 that lies between the peaks 90 and 92, it is possible to crudely separate the objects of interest in the image from the background.

Returning to FIGURE 2B, the computer system computes the threshold that separates objects in the image from the background at step 68. At a step 72, all pixels in the cell image having an intensity less than the threshold value are identified. The results of step 72 are shown in FIGURE 5. The frame image 200 contains numerous objects of interest 202, 204, 206 . . . 226. Some of these objects are cell nuclei, which will be analyzed for the presence of MACs, while other objects are artifacts such as debris, dirt particles, white blood cells, etc., and should be removed from the cell image.

Returning to FIGURE 2B, once the objects in the image have been identified, the computer system calculates the area, shape (sphericity) and optical density of each object according to formulas that are described in further detail below. At a step 76, the computer system removes from memory any objects that cannot be cell nuclei. In the present embodiment of the invention those objects that are not possibly cell nuclei are identified as having an area greater than 2,000 μm^2, an optical density less than 1 c (i.e., less that 1/2 of the overall chromosome count of a normal individual) or a shape or sphericity greater than 4.

The results of step 76 are shown in FIGURE 6 where only a few of the previously identified objects of interest remain. Each of the remaining objects is more likely to be a cell nuclei that is to be examined for a malignancy-associated change.

Again returning to FIGURE 2B, after removing each of the objects that could not be a cell nucleus, the computer system determines whether there are any objects remaining by scanning for dark pixels at step 78. If no objects remain, the computer system returns to step 54, a new image on the slide is captured and steps 54-76 are repeated.

If there are objects remaining in the image after the first attempt at removing artifacts at step 76, the computer system then compensates the image for variations in illumination intensity at step 80. To do this, the computer system recalls a calibration image that was obtained by scanning in a blank slide for the same exposure time that was used for the image of the cells under consideration. The computer system then begins a pixel-by-pixel subtraction of the intensity values of the pixels in the calibration image obtained from the blank slide from the corresponding pixels found in the image obtained from the cell sample. The computer system then adds a value equal to the average illumination of the pixels in the calibration image obtained from

the blank slide to each pixel of the cell image. The result of the addition illuminates the cell image with a uniform intensity.

Once the variations in illumination intensity have been corrected, the computer system attempts to refine the focus of each object of interest in the image at step 82 (FIGURE 2C). The optimum focus is obtained when the object has a minimum size and maximum darkness. The computer system therefore causes the stage to move a predefined amount above the global focus position and then moves in a sequence of descending positions. At each position the CCD camera captures an image of the frame and calculates the area and the intensity of the pixels comprising the remaining objects. Only one image of each object is eventually stored in the computer memory coming from the position in which the pixels comprising the object have the maximum darkness and occupy a minimum area. If the optimum focus is not obtained after a predetermined number of stage positions, then the object is removed from the computer memory and is ignored. Once the optimum focus of the object is determined, the image received from the CCD camera overwrites those pixels that comprise the object under consideration in the computer's memory. The result of the local focusing produces a pseudo-focused image in the computer's memory whereby each object of interest is ultimately recorded at its best possible focus.

At a step 84, the computer system determines whether any in-focus objects in the cell image were found. If not, the computer system returns to step 54 shown in FIGURE 2A whereby the slide is moved to another position and a new image is captured.

Once an image of the object has been focused, the computer system then compensates for local absorbency of light near the object at a step 85. To do this, the computer system analyzes a number of pixels within a box having an area that is larger than the object by two pixels on all sides. An example of such a box is the box 207 shown in FIGURE 6. The computer system then performs a pixel-by-pixel subtraction of the intensity values from a corresponding square in the calibration image obtained from the blank slide. Next the average illumination intensity of the calibration image is added to each pixel in the box surrounding the object. Then the average intensity value for those pixels that are in the box but are not part of the object is determined and this local average value is then subtracted from each pixel in the box that encloses the object.

Once the compensation for absorbency around the object has been made, the computer system then determines a more precise edge of each remaining object in the

cell image at step 86. The steps required to compute the edge are discussed in further detail below.

Having compensated for local absorbency and located the precise edge of the object, the computer system calculates a set of features for each remaining object at a step 87. These feature values are used to further separate artifacts from cell nuclei as well as to identify nuclei exhibiting MACs. The details of the feature calculation are described below.

At a step 88, the computer system runs a classifier that compares the feature values calculated for each object and determines whether the object is an artifact and, if not, whether the object is a nucleus that exhibits MACs.

At a step 90, the pseudo-focus digital image, the feature calculations and the results of the classifier for each in-focus object are stored in the computer's memory.

Finally, at a step 92, the computer system determines whether further scans of the slide are required. As indicated above, because the size of each cell image is much less than the size of the entire slide, a number of cell images are captured to ensure that the slide has been adequately analyzed. Once a sufficient number of cell images have been analyzed, processing stops at step 94. Alternatively, if further scans are required, the computer system loops back to step 54 and a new image of the cell sample is captured.

As indicated above, before the sample can be imaged by the digital microscope, the sample is stained to identify the nuclear material.

FIGURE 4 is a flow chart of the steps used to stain the cell samples. Beginning at a step 100, the cell sample is placed on a slide, air dried and then soaked in a 50% glycerol solution for four minutes. The cell is then washed in distilled water for two minutes at a step 102. At a step 104, the sample is bathed in a 50% ethanol solution for two minutes and again washed with distilled water for two minutes at a step 106. The sample is then soaked in a Bohm-Springer solution for 30 minutes at a step 108 followed by washing with distilled water for one minute at a step 110. At step 112, the sample is soaked in a 5N HCl solution for 45 minutes and rinsed with distilled water for one minute at a step 114. The sample is then stained in a thionine stain for 60 minutes at a step 116 and rinsed with distilled water for one minute at a step 118.

At step 120, the sample is soaked in a bisulfite solution for six minutes followed by a rinse for one minute with distilled water at a step 122. Next, the sample is dehydrated in solutions of 50%, 75% and 100% ethanol for approximately 10 seconds each at a step 124. The sample is then soaked in a final bath of xylene for

one minute at a step 126 before a cover slip is applied at a step 128. After the cell sample has been prepared, it is ready to be imaged by the digital microscope and analyzed as described above.

FIGURES 7A-7F illustrate the manner in which the present invention calculates the precise edge of an object. As shown in FIGURE 7A, an object 230 is comprised of those pixels having an intensity value less than the background/object threshold which is calculated from the histogram and described above. In order to calculate the precise edge, the pixels lying at the original edge of the object are dilated to form a new edge region 242. A second band of pixels lying inside the original edge are also selected to form a second edge region 244. The computer system then assumes that the true edge is somewhere within the annular ring bounded by the edge regions 242 and 244. In the presently preferred embodiment of the invention, the annular ring has a width of approximately ten pixels. To determine the edge, the computer calculates a gradient for each pixel contained in the annular ring. The gradient for each pixel is defined as the sum of the differences in intensity between each pixel and its surrounding eight neighbors. Those pixels having neighbors with similar intensity levels will have a low gradient while those pixels at the edge of the object will have a high gradient.

Once the gradients have been calculated for each pixel in the annular ring, the computer system divides the range of gradients into multiple thresholds and begins removing pixels having lower gradient values from the ring. To remove the pixels, the computer scans the object under consideration in a raster fashion. As shown in FIGURE 7C, the raster scan begins at a point A and continues to the right until reaching a point B. During the first scan, only pixels on the outside edge, i.e., pixels on the edge region 242, are removed. The computer system then scans in the opposite direction by starting, for example, at point D and continuing upwards to point B returning in a raster fashion while only removing pixels on the inside edge region 244 of the annular ring. The computer system then scans in another orthogonal direction--for example, starting at point C and continuing in the direction of point D in a raster fashion, this time only removing pixels on the outside edge region 242. This process continues until no more pixels at that gradient threshold value can be removed.

Pixels are removed from the annular ring subject to the conditions that no pixel can be removed that would break the chain of pixels around the annular ring. Furthermore, adjacent pixels cannot be removed during the same pass of pixel removal. Once all the pixels are removed having a gradient that is less than or equal

to the first gradient threshold, the threshold is increased and the process starts over. As shown in FIGURE 7D, the pixel-by-pixel removal process continues until a single chain of pixels 240' encircles the object in question.

After locating the precise edge of an object, it is necessary to determine whether those pixels that comprise the edge should be included in the object. To do this, the intensity of each pixel that comprises the newly found edge is compared with its eight neighbors. As shown in FIGURE 7E, for example, the intensity of a pixel 246 is compared with its eight surrounding pixels. If the intensity of pixel 246 is less than the intensity of pixel 250, then the pixel 246 is removed from the pixel chain as it belongs to the background. To complete the chain, pixels 248 and 252 are added so that the edge is not broken as shown in FIGURE 7F. After completing the edge relocation algorithm and determining whether each pixel should be included in the object of interest, the system is ready to compute the feature values for the object.

Once the features have been calculated for each in-focus object, the computer system must make a determination whether the object is a cell nucleus that should be analyzed for malignancy-associated changes or is an artifact that should be ignored. As discussed above, the system removes obvious artifacts based on their area, shape (sphericity) and optical density. However, other artifacts may be more difficult for the computer to recognize. To further remove artifacts, the computer system uses a classifier that interprets the values of the features calculated for the object.

As shown in FIGURE 8, a classifier 290 is a computer program that analyzes an object based on its feature values. To construct the classifier two databases are used. The first database 275 contains feature values of objects that have been imaged by the system shown in FIGURE 1 and that have been previously identified by an expert pathologist as non-nuclei, i.e., artifacts. A second database 285 contains the features calculated for objects that have been imaged by the system and that have been previously identified by an expert as cell nuclei. The data in each of these databases is fed into a statistical computer program which uses a stepwise linear discriminant function analysis to derive a discriminant function that can distinguish cell nuclei from artifacts. The classifier is then constructed as a binary decision tree based on thresholds and/or the linear discriminant functions. The binary tree answers a series of questions based on the feature values to determine the identity of an object.

The particular thresholds used in the binary tree are set by statisticians who compare histograms of feature values calculated on known objects. For example, white blood cells typically have an area less than $50\mu m^2$. Because the present invention treats a red blood cell as an artifact, the binary decision tree can contain a

node that compares the area of an object to the 50μm^2 threshold. Objects with an area less than the threshold are ignored while those with an area having a greater area are further analyzed to determine if they are possible MAC cells or artifacts.

In the presently preferred embodiment of the invention, the discriminant functions that separate types of objects are generated by the BMDP program available from BMDP Statistical Software, Inc., of Los Angeles, California. Given the discriminant functions and the appropriate thresholds, the construction of the binary tree classifier is considered routine for one of ordinary skill in the art.

Once the binary tree classifier has been developed, it can be supplied with a set of feature values 292 taken from an unknown object and will provide an indication 294 of whether the object associated with the feature data is most likely an artifact or a cell nucleus.

FIGURE 9 shows how a classifier is used to determine whether a slide exhibits malignancy-associated changes or not. The classifier 300 is constructed using a pair of databases. A first database 302 contains feature values obtained from apparently normal cells that have been imaged by the digital microscope system shown in FIGURE 1 and are known to have come from healthy patients. A second database 304 contains feature values calculated from apparently normal cells that were imaged by the digital microscope system described above and were known to have come from abnormal (i.e., cancer) patients. Again, classifier 300 used in the presently preferred embodiment of the invention is a binary decision tree made up of discriminant functions and/or thresholds that can separate the two groups of cells. Once the classifier has been constructed, the classifier is fed with the feature values 306 that are obtained by imaging cells obtained from a patient whose condition is unknown. The classifier provides a determination 308 of whether the nuclei exhibit MACs or not.

FIGURE 10 is a flow chart of the steps performed by the present invention to determine whether a patient potentially has cancer. Beginning at a step 325, the computer system recalls the features calculated for each in-focus nuclei on the slide. At a step 330, the computer system runs the classifier that identifies MACs based on these features. At a step 332, the computer system provides an indication of whether the nucleus in question is MAC-positive or not. If the answer to step 332 is yes, then an accumulator that totals the number of MAC-positive nuclei for the slide is increased at a step 334. At a step 336, the computer system determines whether all the nuclei for which features have been calculated have been analyzed. If not, the next set of features is recalled at step 338 and the process repeats itself. At a

step 340, the computer system determines whether the frequency of MAC-positive cells on the slide exceeds a predetermined threshold. For example, in a particular preparation of cells (air dried, as is the practice in British Columbia, Canada) to detect cervical cancer, it has been determined that if the total number of MAC-positive epithelial cells divided by the total number of epithelial cells analyzed exceeds 0.45 per slide, then there is an 85% chance that the patient has or will develop cancer. If the frequency of cells exhibiting MACs exceeds the threshold, the computer system can indicate that the patient is healthy at step 342 or likely has or will develop cancer at step 344.

The threshold above which it is likely that a patient exhibiting MACs has or will develop cancer is determined by comparing the MAC scores of a large numbers of patients who did develop cancer and those who did not. As will be appreciated by those skilled in the art, the particular threshold used will depend on the type of cancer to be detected, the equipment used to image the cells, etc.

The MAC detection system of the present invention can also be used to determine the efficacy of cancer treatment. For example, patients who have had a portion of a lung removed as a treatment for lung cancer can be asked to provide a sample of apparently normal cells taken from the remaining lung tissue. If a strong MAC presence is detected, there is a high probability that the cancer will return. Conversely, the inventors have found that the number of MAC cells decreases when a cancer treatment is effective.

As described above, the ability of the present invention to detect malignancy-associated changes depends on the values of the features computed. The following is a list of the features that is currently calculated for each in-focus object.

I.2 Coordinate Systems, Jargon and Notation

Each image is a rectangular array of square pixels that contains within it the image of an (irregularly shaped) object, surrounded by background. Each pixel $P_{i,j}$ is an integer representing the photometric value (gray scale) of a corresponding small segment of the image, and may range from 0 (completely opaque) to 255 (completely transparent). The image rectangle is larger than the smallest rectangle that can completely contain the object by at least two rows, top and bottom, and two columns left and right, ensuring that background exists all around the object. The rectangular image is a matrix of pixels, $P_{i,j}$, spanning $i = 1, L$ columns and $j = 1, M$ rows and with the upper left-hand pixel as the coordinate system origin, $i = j = 1$.

The region of the image that is the object is denoted by its characteristic function, Ω; this is also sometimes called the "object mask" or, simply, the "mask." For some features, it makes sense to dilate the object mask by one pixel all around the object; this mask is denoted Ω^+. Similarly, an eroded mask is denoted Ω^-. The object mask is a binary function:

$$\Omega = \left(\Omega_{1,1}, \Omega_{1,2}, \ldots \Omega_{i,j}, \ldots \Omega_{L,M}\right) \tag{1}$$

where

$$\Omega_{i,j} = \begin{cases} 1 \; if \; (i,j) \in object \\ 0 \; if \; (i,j) \notin object \end{cases}$$

and where "*(i,j)* $\in$ object" means pixels at coordinates: *(i, j)* are part of the object, and "*(i,j)* $\notin$ object" means pixels at coordinates: *(i, j)* are not part of the object.

II Morphological Features

Morphological features estimate the image area, shape, and boundary variations of the object.

II.1 area

The area, A, is defined as the total number of pixels belonging to the object, as defined by the mask, Ω:

$$\text{area} = A = \sum_{i=1}^{L} \sum_{j=1}^{M} \Omega_{ij} \tag{2}$$

where *i*, *j* and Ω are defined in Section I.2 above.

II.2 x_centroid, y_centroid

The x_centroid and y_centroid are the coordinates of the geometrical center of the object, defined with respect to the image origin (upper-left hand corner):

$$x\_centroid = \frac{\sum_{i=1}^{L}\sum_{j=1}^{M} i \cdot \Omega_{i,j}}{A} \tag{3}$$

$$y\_centroid = \frac{\sum_{i=1}^{L}\sum_{j=1}^{M} i \cdot \Omega_{i,j}}{A} \tag{4}$$

where i and j are the image pixel coordinates and Ω is the object mask, as defined in Section 1.2 above, and A is the object area.

II.3 mean_radius, max_radius

The mean_radius and max_radius features are the mean and maximum values of the length of the object's radial vectors from the object centroid to its 8 connected edge pixels:

$$mean\_radius = \bar{r} = \frac{\sum_{k=1}^{N} r_k}{N} \tag{5}$$

$$max\_radius = max(r_k) \tag{6}$$

where r_k is the k^{th} radial vector, and N is the number of 8 connected pixels on the object edge.

II.4 var_radius

The var_radius feature is the variance of length of the object's radius vectors, as defined in Section II.3.

$$var\_radius = \frac{\sum_{k=1}^{N} (r_k - \bar{r})^2}{N-1} \tag{7}$$

where r_k is the k^{th} radius vector, $\bar{r}$ is the mean_radius, and N is the number of 8 connected edge pixels.

II.5 sphericity

The sphericity feature is a shape measure, calculated as a ratio of the radii of two circles centered at the object centroid (defined in Section II.2 above). One circle is the largest circle that is fully inscribed inside the object perimeter, corresponding to the absolute minimum length of the object's radial vectors. The other circle is the minimum circle that completely circumscribes the object's perimeter, corresponding to the absolute maximum length of the object's radial vectors. The maximum sphericity value: 1 is given for a circular object:

$$sphericity = \frac{min\_radius}{max\_radius} = \frac{min(r_k)}{max(r_k)} \tag{8}$$

where r_k is the k^{th} radius vector.

II.6 eccentricity

The eccentricity feature is a shape function calculated as the square root of the ratio of maximal and minimal eigenvalues of the second central moment matrix of the object's characteristic function, Ω:

$$eccentricity = \sqrt{\frac{\lambda_1}{\lambda_2}} \tag{9}$$

where λ_1 and λ_2 are the maximal and minimal eigenvalues, respectively, and the characteristic function, Ω, as given by Equation 1. The second central moment matrix is calculated as:

$$\begin{bmatrix} x_{moment2} & xy_{crossmoment2} \\ xy_{crossmoment2} & y_{moment2} \end{bmatrix} = \tag{10}$$

$$\begin{bmatrix} \sum_{i=1}^{L}\sum_{j=1}^{M}\left(i-\frac{\sum_{i=1}^{L} i\cdot\Omega_{i,j}}{L}\right) & \sum_{i=1}^{L}\sum_{j=1}^{M}\left(i-\frac{\sum_{i=1}^{L} i\cdot\Omega_{i,j}}{L}\right)\left(j-\frac{\sum_{j=1}^{M} j\cdot\Omega_{i,j}}{M}\right) \\ \sum_{i=1}^{L}\sum_{j=1}^{M}\left(i-\frac{\sum_{i=1}^{L} i\cdot\Omega_{i,j}}{L}\right)\left(j-\frac{\sum_{j=1}^{M} j\cdot\Omega_{i,j}}{M}\right) & \sum_{i=1}^{L}\sum_{j=1}^{M}\left(j-\frac{\sum_{j=1}^{M} j\cdot\Omega_{i,j}}{M}\right)^2 \end{bmatrix}$$

Eccentricity may be interpreted as the ratio of the major axis to minor axis of the "best fit" ellipse which describes the object, and gives the minimal value 1 for circles.

II.7 inertia_shape

The inertia_shape feature is a measure of the "roundness" of an object calculated as the moment of inertia of the object mask, normalized by the area squared, to give the minimal value 1 for circles:

$$inertia\_shape = \frac{2\pi\sum_{i=1}^{L}\sum_{j=1}^{M} R_{i,j}^2\Omega_{i,j}}{A^2} \qquad (11)$$

where $R_{i,j}$ is the distance of the pixel, $P_{i,j}$, to the object centroid (defined in Section II.2), and A is the object area, and Ω is the mask defined by Equation 1.

II.8 compactness

The compactness feature is another measure of the object's "roundness." It is calculated as the perimeter squared divided by the object area, giving the minimal value 1 for circles:

$$compactness = \frac{P^2}{4\pi A} \qquad (12)$$

where P is the object perimeter and A is the object area. Perimeter is calculated from boundary pixels (which are themselves 8 connected) by considering their 4 connected neighborhood:

$$P = N_1 + \sqrt{2}N_2 + 2N_3 \quad (13)$$

where N_1 is the number of pixels on the edge with 1 non-object neighbor, N_2 is the number of pixels on the edge with 2 non-object neighbors, and N_3 is the number of pixels on the edge with 3 non-object neighbors.

II.9 cell_orient

The cell_orient feature represents the object orientation measured as a deflection of the main axis of the object from the y direction:

$$\text{cell\_orient} = \frac{180}{\pi}\left(\frac{\pi}{2} + \arctan\left[\frac{(\lambda_1 - y_{moment2})}{xy_{cross\_moment2}}\right]\right) \quad (14)$$

where $y_{moment2}$ and $xy_{crossmoment2}$ are the second central moments of the characteristic function Ω defined by Equation 1 above , and λ_1 is the maximal eigenvalue of the second central moment matrix of that function (see Section II.6 above). The main axis of the object is defined by the eigenvector corresponding to the maximal eigenvalue. A geometrical interpretation of the cell_orient is that it is the angle (measured in a clockwise sense) between the y axis and the "best fit" ellipse major axis.

For slides of cell suspensions, this feature should be meaningless, as there should not be any *a priori* preferred cellular orientation. For histological sections, and possibly smears, this feature may have value. In smears, for example, debris may be preferentially elongated along the slide long axis.

II.10 elongation

Features in Sections II.10 to II.13 are calculated by sweeping the radius vector (from the object centroid, as defined in Section II.2, to object perimeter) through 128 discrete equal steps (i.e., an angle of $2\pi/128$ per step), starting at the top left-most object edge pixel, and sweeping in a clockwise direction. The function is interpolated from an average of the object edge pixel locations at each of the 128 angles.

The elongation feature is another measure of the extent of the object along the principal direction (corresponding to the major axis) versus the direction normal to it. These lengths are estimated using Fourier Transform coefficients of the radial function of the object:

$$elongation = \frac{a_0 + 2\sqrt{a_2^2 + b_2^2}}{a_0 - 2\sqrt{a_2^2 + b_2^2}} \tag{15}$$

where a_2, b_2 are Fourier Transform coefficients of the radial function of the object, $r(\theta)$, defined by:

$$r(\theta) = \frac{a_0}{2} + \sum_{n=1}^{m} a_n \cos(n\theta) + \sum_{n=1}^{m} b_n \sin(n\theta) \tag{16}$$

II.11 freq_low_fft

The freq_low_fft gives an estimate of coarse boundary variation, measured as the energy of the lower harmonics of the Fourier spectrum of the object's radial function (from 3rd to 11th harmonics):

$$freq\_low\_fft = \sum_{n=3}^{11} (a_n^2 + b_n^2) \tag{17}$$

where a_n, b_n are Fourier Transform coefficients of the radial function, defined in Equation 16.

II.12 freq_high_fft

The freq_high_fft gives an estimate of the fine boundary variation, measured as the energy of the high frequency Fourier spectrum (from 12th to 32nd harmonics) of the object's radial function:

$$\text{freq\_high\_fft} = \sum_{n=12}^{32} \left(a_n^2 + b_n^2 \right) \tag{18}$$

where a_n, b_n are Fourier Transform coefficients of the n^{th} harmonic, defined by Equation 16.

II.13 harmon01_fft, ..., harmon32_fft

The harmon01_fft, ... harmon32_fft features are estimates of boundary variation, calculated as the magnitude of the Fourier Transform coefficients of the object radial function for each harmonic 1 - 32:

$$\text{harmon}\,n\_\text{fft} = \sqrt{a_n^2 + b_n^2} \tag{19}$$

where a_n, b_n are Fourier Transform coefficients of the n^{th} harmonic, defined by Equation 16.

III Photometric Features

Photometric features give estimations of absolute intensity and optical density levels of the object, as well as their distribution characteristics.

III.1 DNA_Amount

DNA_Amount is the "raw" (unnormalized) measure of the integrated optical density of the object, defined by a once dilated mask, Ω^+:

$$DNA\_Amount = \sum_{i=1}^{L}\sum_{j=1}^{M} OD_{i,j}\Omega^+_{i,j} \tag{20}$$

where the once dilated mask, Ω^+ is defined in Section I.2 and OD is the optical density, calculated according to [12]:

$$OD_{i,j} = log_{10} I_B - log_{10} I_{i,j} \tag{21}$$

where I_B is the intensity of the local background, and I_{ij} is the intensity of the i,j th pixel.

III.2 DNA_Index

DNA_Index is the normalized measure of the integrated optical density of the object:

$$DNA\_Index = \frac{DNA\_Amount}{iod_{norm}} \tag{22}$$

where iod_{norm} is the mean value of the DNA amount for a particular object population from the slide (e.g., leukocytes).

III.3 var_intensity, mean_intensity

The var_intensity and mean_intensity features are the variance and mean of the intensity function of the object, I, defined by the mask, Ω:

$$\text{var\_intensity} = \frac{\sum_{i=1}^{L}\sum_{j=1}^{M}(I_{i,j}\Omega_{i,j} - \bar{I})^2}{A-1} \tag{23}$$

where A is the object area, Ω is the object mask defined in Equation 1, and $\bar{I}$ is given by:

$$\bar{I} = \frac{\sum_{i=1}^{L}\sum_{j=1}^{M} I_{i,j}\Omega_{i.j}}{A} \tag{24}$$

$\bar{I}$ is the "raw" (unnormalized) mean intensity.
mean intensity is normalized against iod_{norm} defined in Section III.2:

$$\text{mean\_intensity} = \bar{I}\frac{(iod_{norm})}{100} \tag{25}$$

III.4 OD_maximum

OD_maximum is the largest value of the optical density of the object, normalized to iod_{norm}, as defined in Section III.2 above:

$$OD\_\text{maximum} = \max(OD_{i,j})\left(\frac{100}{iod_{norm}}\right) \tag{26}$$

III.5 OD_variance

OD_variance is the normalized variance (second moment) of optical density function of the object:

$$OD\_\text{variance} = \frac{\sum_{i=1}^{L}\sum_{j=1}^{M}(OD_{i,j}\Omega_{i,j} - \overline{OD})^2}{(A-1)\overline{OD}^2} \tag{27}$$

where Ω is the object mask as defined in Section 1.2, $\overline{OD}$ is the mean value of the optical density of the object:

$$\overline{OD} = \left(\frac{\sum_{i=1}^{L} \sum_{j=1}^{M} OD_{i,j} \Omega_{i,j}}{A} \right)$$

and A is the object area (total number of pixels). The variance is divided by the square of the mean optical density in order to make the measurement independent of the staining intensity of the cell.

III.6 OD_skewness

The OD_skewness feature is the normalized third moment of the optical density function of the object:

$$OD\_\text{skewness} = \frac{\sum_{i=1}^{L} \sum_{j=1}^{M} (OD_{i,j} \Omega_{i,j} - \overline{OD})^3}{(A-1)\left(\sum_{i=1}^{L} \sum_{j=1}^{M} (OD_{i,j} \Omega_{i,j} - \overline{OD})^2 \right)^{\frac{3}{2}}} \quad (28)$$

where Ω is the object mask as defined in Section 1.2, $\overline{OD}$ is the mean value of the optical density of the object and A is the object area (total number of pixels).

III.7 OD_kurtosis

OD_kurtosis is the normalized fourth moment of the optical density function of the object:

$$OD\_kurtosis = \frac{\sum_{i=1}^{L} \sum_{j=1}^{M} (OD_{i,j} \Omega_{i,j} - \overline{OD})^4}{(A-1)\left(\sum_{i=1}^{L} \sum_{j=1}^{M} (OD_{i,j} \Omega_{i,j} - \overline{OD})^2 \right)^2} \quad (29)$$

where Ω is the object mask as defined in Section 1.2, $\overline{OD}$ is the mean value of the optical density of the object and A is the object area.

IV Discrete Texture Features

The discrete texture features are based on segmentation of the object into regions of low, medium and high optical density. This segmentation of the object into low, medium and high density regions is based on two thresholds: optical density high threshold and optical density medium threshold. These thresholds are scaled to the sample's iod_{norm} value, based on the DNA amount of a particular subset of objects (e.g., lymphocytes), as described in Section III.2 above.

By default, these thresholds have been selected such that the condensed chromatin in leukocytes is high optical density material. The second threshold is located half way between the high threshold and zero.

The default settings from which these thresholds are calculated are stored in the computer as:

CHROMATIN_HIGH_THRES = 36

CHROMATIN_MEDIUM_THRES = 18

A^{high} is the area of the pixels having an optical density between 0 and 18, $A^{med.}$ is the area of the pixels having an optical density between 18 and 36 and A^{low} is the area of the pixels having an optical density greater than 36. Together the areas A^{high}, A^{med} and A^{low} sum to the total area of the object. The actual thresholds used are these parameters, divided by 100, and multiplied by the factor $iod_{norm}/100$.

In the following discussion, Ω^{low}, Ω^{med}, and Ω^{high} are masks for low-, medium-, and high-optical density regions of the object, respectively, defined in analogy to Equation 1.

IV.1 lowDNAarea, medDNAarea, hiDNAarea

These discrete texture features represent the ratio of the area of low, medium, and high optical density regions of the object to the total object area:

$$\text{lowDNAarea} = \frac{\sum_{i=1}^{L}\sum_{j=1}^{M}\Omega_{i,j}^{low}}{\sum_{i=1}^{L}\sum_{j=1}^{M}\Omega_{i,j}} = \frac{A^{low}}{A} \qquad (30)$$

$$\text{medDNAarea} = \frac{\sum_{i=1}^{L}\sum_{j=1}^{M}\Omega_{i,j}^{med}}{\sum_{i=1}^{L}\sum_{j=1}^{M}\Omega_{i,j}} = \frac{A^{med}}{A} \tag{31}$$

$$\text{hiDNAarea} = \frac{\sum_{i=1}^{L}\sum_{j=1}^{M}\Omega_{i,j}^{hi}}{\sum_{i=1}^{L}\sum_{j=1}^{M}\Omega_{i,j}} = \frac{A^{hi}}{A} \tag{32}$$

where Ω is the object mask as defined in Equation 1, and A is the object area.

IV.2 lowDNAamnt, medDNAamnt, hiDNAamnt

These discrete texture features represent the total extinction ratio for low, medium, and high optical density regions of the object, calculated as the value of the integrated optical density of the low-, medium-, and high-density regions, respectively, divided by the total integrated optical density:

$$\text{lowDNAamnt} = \frac{\sum_{i=1}^{L}\sum_{j=1}^{M} OD_{i,j}\Omega_{i,j}^{low}}{\sum_{i=1}^{L}\sum_{j=1}^{M} OD_{i,j}\Omega_{i,j}} \tag{33}$$

$$\text{medDNAamnt} = \frac{\sum_{i=1}^{L}\sum_{j=1}^{M} OD_{i,j}\Omega_{i,j}^{med}}{\sum_{i=1}^{L}\sum_{j=1}^{M} OD_{i,j}\Omega_{i,j}} \tag{34}$$

$$\text{hiDNAamnt} = \frac{\sum_{i=1}^{L}\sum_{j=1}^{M} OD_{i,j}\Omega_{i,j}^{hi}}{\sum_{i=1}^{L}\sum_{j=1}^{M} OD_{i,j}\Omega_{i,j}} \tag{35}$$

where Ω is the object mask as defined in Equation 1, and OD is the optical density as defined by Equation 21.

IV.3 lowDNAcomp, medDNAcomp, hiDNAcomp, mhDNAcomp

These discrete texture features are characteristic of the compactness of low-, medium-, high-, and combined medium- and high-density regions, respectively, treated as single (possibly disconnected) objects. They are calculated as the perimeter squared of each region, divided by 4π (area) of the region.

$$\text{lowDNAcomp} = \frac{(P^{low})^2}{4\pi A^{low}} \tag{36}$$

$$\text{medDNAcomp} = \frac{(P^{med})^2}{4\pi A^{med}} \tag{37}$$

$$\text{hiDNAcomp} = \frac{(P^{hi})^2}{4\pi A^{hi}} \tag{38}$$

$$\text{mhDNAcomp} = \frac{(P_{med} + P_{hi})^2}{4\pi (A^{med} + A^{hi})} \tag{39}$$

where P is the perimeter of each of the optical density regions, defined in analogy to Equation 13, and A is the region area, defined in analogy to Equation 2.

IV.4 low_av_dst, med_av_dst, hi_av_dst, mh_av_dst

These discrete texture features represent the average separation between the low-, medium-, high-, and combined medium- and high-density pixels from the center of the object, normalized by the object mean_radius.

$$low\_av\_dst = \frac{\sum_{i=1}^{L}\sum_{j=1}^{M} R_{i,j}\Omega_{i,j}^{low}}{A^{low} \cdot mean\_radius} \tag{40}$$

$$med\_av\_dst = \frac{\sum_{i=1}^{L}\sum_{j=1}^{M} R_{i,j}\Omega_{i,j}^{med}}{A^{med} \cdot mean\_radius} \tag{41}$$

$$hi\_av\_dst = \frac{\sum_{i=1}^{L}\sum_{j=1}^{M} R_{i,j}\Omega_{i,j}^{hi}}{A^{hi} \cdot mean\_radius} \tag{42}$$

$$mh\_av\_dst = \frac{\sum_{i=1}^{L}\sum_{j=1}^{M} R_{i,j}\Omega_{i,j}^{med} + \sum_{i=1}^{L}\sum_{j=1}^{M} R_{i,j}\Omega_{i,j}^{hi}}{(A^{med} + A^{hi}) \cdot mean\_radius} \quad (43)$$

where $R_{i,j}$ is defined in Section II.7 as the distance from pixel $P_{i,j}$ to the object centroid (defined in Section II.2), and the object mean_radius is defined by Equation 5.

IV.5 lowVSmed_DNA, lowVShigh_DNA, lowVSmh_DNA

These discrete texture features represent the average extinction ratios of the low- density regions, normalized by the medium-, high-, and combined medium- and high-average extinction values, respectively. They are calculated as the mean optical density of the medium-, high-, and combined medium- and high-density clusters divided by the mean optical density of the low density clusters.

$$lowVSmed\_DNA = \left(\frac{\sum_{i=1}^{L}\sum_{j=1}^{M} OD_{i,j}\Omega_{i,j}^{med}}{A^{med}} \right) \div \left(\frac{\sum_{i=1}^{L}\sum_{j=1}^{M} OD_{i,j}\Omega_{i,j}^{low}}{A^{low}} \right) \quad (44)$$

$$lowVShi\_DNA = \left(\frac{\sum_{i=1}^{L}\sum_{j=1}^{M} OD_{i,j}\Omega_{i,j}^{hi}}{A^{hi}} \right) \div \left(\frac{\sum_{i=1}^{L}\sum_{j=1}^{M} OD_{i,j}\Omega_{i,j}^{low}}{A^{low}} \right) \quad (45)$$

$$lowVSmh\_DNA = \left(\frac{\sum_{i=1}^{L}\sum_{j=1}^{M} OD_{i,j}\Omega_{i,j}^{med} + \sum_{i=1}^{L}\sum_{j=1}^{M} OD_{i,j}\Omega_{i,j}^{hi}}{A^{med} + A^{hi}} \right) \div \left(\frac{\sum_{i=1}^{L}\sum_{j=1}^{M} OD_{i,j}\Omega_{i,j}^{low}}{A^{low}} \right) \quad (46)$$

where OD is the region optical density defined in analogy to Equation 21, Ω is the region mask, defined in analogy to Equation 1, and A is the region area, defined in analogy to Equation 2.

IV.6 low_den_obj, med_den_obj, high_den_obj

These discrete texture features are the numbers of discrete 8-connected subcomponents of the objects consisting of more than one pixel of low, medium, and high density.

IV.7 low_cntr_mass, med__cntr_mass, high_cntr_mass

These discrete texture features represent the separation between the geometric center of the low, medium, and high optical density clusters (treated as if they were single objects) and the geometric center of the whole object, normalized by its mean_radius.

$$\text{low\_cntr\_mass} = \left[\left(\frac{\sum_{i=1}^{L}\sum_{j=1}^{M} i \cdot \Omega_{i,j}^{low}}{A^{low}} - x\_centroid \right)^2 + \left(\frac{\sum_{i=1}^{L}\sum_{j=1}^{M} j \cdot \Omega_{i,j}^{low}}{A^{low}} - y\_centroid \right)^2 \right]^{\frac{1}{2}} \div (mean\_radius) \tag{47}$$

$$\text{med\_cntr\_mass} = \left[\left(\frac{\sum_{i=1}^{L}\sum_{j=1}^{M} i \cdot \Omega_{i,j}^{med}}{A^{med}} - x\_centroid \right)^2 + \left(\frac{\sum_{i=1}^{L}\sum_{j=1}^{M} j \cdot \Omega_{i,j}^{med}}{A^{med}} - y\_centroid \right)^2 \right]^{\frac{1}{2}} \div (mean\_radius) \tag{48}$$

$$\text{hi\_cntr\_mass} = \left[\left(\frac{\sum_{i=1}^{L}\sum_{j=1}^{M} i \cdot \Omega_{i,j}^{hi}}{A^{hi}} - x\_centroid \right)^2 + \left(\frac{\sum_{i=1}^{L}\sum_{j=1}^{M} j \cdot \Omega_{i,j}^{hi}}{A^{hi}} - y\_centroid \right)^2 \right]^{\frac{1}{2}} \div (mean\_radius) \tag{49}$$

where mean_radius of the object is defined by Equation 5, the object's centroid is defined in Section II.2, Ω is the region mask defined in analogy to Equation 1, and A is the region area defined in analogy to Equation 2.

V Markovian Texture Features

Markovian texture features are defined from the co-occurrence matrix, $\Delta_{\lambda,\mu}$ of object pixels. Each element of that matrix stands for the conditional probability of the pixel of grey level λ occurring next (via 8-connectedness) to a pixel of grey level μ, where λ, μ are row and column indices of the matrix, respectively. However, the computational algorithms used here for the calculation of Markovian texture features uses so-called sum and difference histograms: H_l^s *and* H_m^d, where H_l^s is the probability of neighboring pixels having grey levels which sum to l, and H_m^d is the probability of neighboring pixels having grey level differences of m, where an 8-connected neighborhood is assumed. Values of grey levels, l, m, used in the sum and difference histogram are obtained by quantization of the dynamic range of each individual object into 40 levels.

For completeness, the formulae that follow for Markovian texture features include both the conventional formulae and the computational formulae actually used.

V.1 entropy

The entropy feature represents a measure of "disorder" in object grey level organization: large values correspond to very disorganized distributions, such as a "salt and pepper" random field:

$$entropy = \sum_{\lambda}\sum_{\mu} \Delta_{\lambda,\mu}\, log_{10}\, \Delta_{\lambda,\mu} \quad (conventional)$$

$$\text{entropy} = -\sum_{l} H_l^s \log_{10} H_l^s - \sum_{m} H_m^d \log_{10} H_m^d \quad (computational) \qquad (50)$$

V.2 energy

The energy feature gives large values for an object with a spatially organized grey scale distribution. It is the opposite of entropy, giving large values to an object with large regions of constant grey level:

$$\text{energy} = \sum_{\lambda}\sum_{\mu} \Delta_{\lambda,\mu}^2 \quad (conventional)$$

$$\text{energy} = \sum_{l} (H_l^s) + \sum_{m} (H_m^d)^2 \quad (computational) \qquad (51)$$

V.3 contrast

The contrast feature gives large values for an object with frequent large grey scale variations:

$$\text{contrast} = \sum_{\lambda}\sum_{\mu}(\lambda-\mu)^2\Delta_{\lambda,\mu} \quad (\textit{conventional})$$

$$\text{contrast} = \sum_{m} m^2 H_m^d \quad (\textit{computational}) \tag{52}$$

V.4 correlation

A large value for correlation indicates an object with large connected subcomponents of constant grey level and with large grey level differences between adjacent components:

$$\text{correlation} = \sum_{\lambda}\sum_{\mu}(\lambda-\overline{I^q})(\mu-\overline{I^q})\Delta_{\lambda,\mu} \quad (\textit{conventional})$$

$$\text{correlation} = \frac{1}{2}\left(\sum_{\lambda}(l-2\overline{I^q})H_l^s - \sum_{m} m^2 H_m^d\right) \quad (\textit{computational}) \tag{53}$$

where $\overline{I^q}$ is the mean intensity of the object calculated for the grey scale quantized to 40 levels.

V.5 homogeneity

The homogeneity feature is large for objects with slight and spatially smooth grey level variations:

$$\text{homogeneity} = \sum_{\lambda}\sum_{\mu}\frac{1}{1+(\lambda-\mu)^2}\Delta_{\lambda,\mu} \quad (\textit{conventional})$$

$$\text{homogeneity} = \sum_{m}\frac{1}{(1+m)^2}H_m^d \quad (\textit{computational}) \tag{54}$$

V.6 cl_shade

The cl_shade feature gives large absolute values for objects with a few distinct clumps of uniform intensity having large contrast with the rest of the object. Negative values correspond to dark clumps against a light background while positive values indicate light clumps against a dark background:

$$\text{cl\_shade} = \sum_{\lambda}\sum_{\mu}(\lambda+\mu-2\overline{I^q})^3\Delta_{\lambda,\mu} \quad (\textit{conventional})$$

$$\text{cl\_shade} = \frac{\sum_{l}(l-2\overline{I^q})^3 H_l^s}{\left(\sum_{l}(l-2\overline{I^q})^2 H_l^s\right)^{\frac{3}{2}}} \quad (\textit{computational}) \qquad (55)$$

V.7 cl_prominence

The feature cl_prominence measures the darkness of clusters.

$$\text{cl\_prominence} = \sum_{\lambda}\sum_{\mu}(\lambda+\mu-2\overline{I^q})^4\Delta_{\lambda,\mu} \quad (\textit{conventional})$$

$$\text{cl\_prominence} = \frac{\sum_{l}(l-2\overline{I^q})^4 H_l^s}{\left(\sum_{l}(l-2\overline{I^q})^2 H_l^s\right)^{2}} \quad (\textit{computational}) \qquad (56)$$

VI Non-Markovian Texture Features

These features describe texture in terms of global estimation of grey level differences of the object.

VI.1 den_lit_spot, den_drk_spot

These are the numbers of local maxima and local minima, respectively, of the object intensity function based on the image averaged by a 3 x 3 window, and divided by the object area.

$$\text{den\_lit\_spot} = \frac{\sum_{i'=1}^{L}\sum_{j'=1}^{M}\delta_{i',j'}^{\max}}{A} \tag{57}$$

and

$$\text{den\_drk\_spot} = \frac{\sum_{i'=1}^{L}\sum_{j'=1}^{M}\delta_{i',j'}^{\min}}{A} \tag{58}$$

where

$$\delta_{i',j'}^{max} = \begin{cases} 1 \text{ if there exists a local maximum of } I'_{i',j'} \text{ with value } max_{i',j'} \\ 0 \text{ otherwise} \end{cases}$$

and

$$\delta_{i',j'}^{min} = \begin{cases} 1 \text{ if there exists a local minimum of } I'_{i',j'} \text{ with value } min_{i',j'} \\ 0 \text{ otherwise} \end{cases}$$

and where

$$I'_{i',j'} = \frac{1}{9}\sum_{i=i'-1}^{i'+1}\sum_{j=j'-1}^{j'+1} I_{i,j}\Omega_{i,j}$$

and I is the object intensity, Ω is the object mask, and A is the object area.

VI.2 range_extreme

This is the intensity difference between the largest local maximum and the smallest local minimum of the object intensity function, normalized against the slide DNA amount, iod_{norm}, defined in Section III.2. The local maxima, $max_{i',j'}$ and minima, $min_{i',j'}$, are those in Section VI.1 above.

$$\text{range\_extreme} = (max(max_{i',j'}) - (min(min_{i,j}))\left(\frac{100}{iod_{norm}}\right) \qquad (59)$$

VI.3 range_average

This is the intensity difference between the average intensity of the local maxima and the average intensity of the local minima, normalized against the slide DNA amount value, iod_{norm}, defined in Section III.2 above. The local maxima, $max_{i',j'}$ and minima, $min_{i',j'}$, values used are those from Section VI.1 above.

$$\text{range\_average} = \left(\frac{\sum_{i'=1}^{L}\sum_{j'=1}^{M} max_{i',j'}}{\sum_{i'=1}^{L}\sum_{j'=1}^{M}\delta_{i',j'}^{max}} - \frac{\sum_{i'=1}^{L}\sum_{j'=1}^{M} min_{i',j'}}{\sum_{i'=1}^{L}\sum_{j'=1}^{M}\delta_{i',j'}^{min}}\right)\frac{100}{iod_{norm}} \qquad (60)$$

VI.4 center_of_gravity

The center_of_gravity feature represents the distance from the geometrical center of the object to the "center of mass" of the optical density function, normalized by the mean_radius of the object:

$$\text{center\_of\_gravity} = \frac{\left[\left(\frac{\sum_{i=1}^{L}\sum_{j=1}^{M} i\cdot OD_{i,j}\Omega_{i,j}}{\sum_{i=1}^{L}\sum_{j=1}^{M} OD_{i,j}\Omega_{i,j}} - x\_centroid\right)^2 + \left(\frac{\sum_{i=1}^{L}\sum_{j=1}^{M} j\cdot OD_{i,j}\Omega_{i,j}}{\sum_{i=1}^{L}\sum_{j=1}^{M} OD_{i,j}\Omega_{i,j}} - y\_centroid\right)\right]}{mean\_radius} \qquad (61)$$

This gives a measure of the nonuniformity of the OD distribution.

VII Fractal Texture Features

The fractal texture features are based on the area of the three-dimensional surface of the object's optical density represented essentially as a three-dimensional bar graph, with the vertical axis representing optical density, and the horizontal axes representing the x and y spatial coordinates. Thus, each pixel is assigned a unit area in the x - y plane plus the area of the sides of the three-dimensional structure proportional to the change in the pixel optical density with respect to its neighbors. The largest values of fractal areas correspond to large objects containing small subcomponents with high optical density variations between them.

The difference between fractal1_area and fractal2_area is that these features are calculated on different scales: the second one is based on an image in which four pixels are averaged into a single pixel, thereby representing a change of scale of fractal1_area. This calculation needs the additional mask transformation: $\Omega_{i2,j2}$ represents the original mask Ω with 4 pixels mapped into one pixel and any square of 4 pixels not completely consisting of object pixels is set to zero. $\Omega i,j$ represents $\Omega_{i2,j2}$ expanded by 4 so that each pixel in $\Omega_{i2,j2}$ is 4 pixels in $\Omega i,j$.

VII.1 fractal1_area

$$\text{fractal 1\_ area} = \sum_{i=2}^{L}\sum_{j=2}^{M}(\left|OD^{*}_{i,j} - OD^{*}_{i,j-1}\right| + \left|OD^{*}_{i,j} - OD^{*}_{i-1,j}\right| + 1)\Omega_{i,j} \qquad (62)$$

where $OD^{*}_{i,j}$ is the optical density function of the image scaled by a factor common to all images such that the possible optical density values span 256 levels.

VII.2 fractal2_area

This is another fractal dimension, but based on an image in which four pixel squares are averaged into single pixels, thereby representing a change of scale of fractal1_area in Section VII.1 above.

$$\text{fractal2\_area} = \sum_{i_2=2}^{L_2}\sum_{j_2=2}^{M_2}(\left|OD^{*}_{i2,j2} - OD^{*}_{i_2,j_2-1}\right| + \left|OD^{*}_{i_2,j_2} - OD^{*}_{i_2-1,j_2}\right| + 1)\Omega_{i_2,j_2} \qquad (63)$$

where, $L_2 = \left[\frac{L}{2}\right], M_2 = \left[\frac{M}{2}\right]$, with L_2, M_2 as integers, and $OD^{*}_{i2,j2}$ is a scaled optical density function of the image, with 4 pixels averaged into one.

VII.3 fractal_dimen

The fractal_dimen feature is calculated as the difference between logarithms of fractal1_area and fractal2_area, divided by log 2. This varies from 2 to 3 and gives a measure of the "fractal behavior" of the image, associated with a rate at which measured surface area increases at finer and finer scales.

$$\text{fractal\_dimen} = \frac{\log_{10}(\textit{fractal1\_area}) - \log_{10}(\textit{fractal2\_area})}{\log_{10} 2} \qquad (64)$$

VIII Run Length Texture Features

Run length features describe texture in terms of grey level runs, representing sets of consecutive, collinear pixels having the same grey level value. The length of the run is the number of pixels in the run. These features are calculated over the image with intensity function values transformed into 8 levels.

The run length texture features are defined using grey level length matrices, $\Re^{\Theta}_{p,q}$ for each of the four principal directions: θ = 0°, 45°, 90°, 135°, where the directions are defined clockwise with respect to the positive x-axis. Note: As defined here, the run length texture features are not rotationally invariant, and therefore cannot, in general, be used separately since for most samples there will be no *a priori* preferred direction for texture. For example, for one cell, a run length feature may be oriented at 45°, but at 90° in the next; in general, these are completely equivalent. Each element of matrix $\Re^{\Theta}_{p,q}$ specifies the number of times that the object contains a run of length q, in a given direction, Θ, consisting of pixels lying in grey level range, p (out of 8 grey levels). Let $N^g = 8$ be the number of grey levels, and N^r be the number of different run lengths that occur in the object; then the run length features are described as follows:

VIII.1 short0_runs, short45_runs, short90_runs, short135_runs

These give large values for objects in which short runs, oriented at 0°, 45°, 90°, or 135°, dominate.

$$\textit{short}\Theta\textit{\_runs} = \frac{\sum_{p=1}^{N^g}\sum_{q=1}^{N^r}\frac{\Re^{\Theta}_{p,q}}{q^2}}{\sum_{p=1}^{N^g}\sum_{q=1}^{N^r}\Re^{\Theta}_{p,q}} \qquad (65)$$

VIII.2 long0_runs, long45_runs, long90_runs, long135_runs

These give large values for objects in which long runs, oriented at 0°, 45°, 90°, or 135°, dominate.

$$\text{long}\theta\_\text{runs} = \frac{\sum_{p=1}^{N^g}\sum_{q=1}^{N^r} q^2 \Re_{p,q}^{\Theta}}{\sum_{p=1}^{N^g}\sum_{q=1}^{N^r} \Re_{p,q}^{\Theta}} \tag{66}$$

VIII.3 grey0_level, grey45_level, grey90_level, grey135_level

These features estimate grey level nonuniformity, taking on their lowest values when runs are equally distributed throughout the grey levels.

$$\text{grey}\theta\_\text{level} = \frac{\sum_{p=1}^{N^g}\left(\sum_{q=1}^{N^r} \Re_{p,q}^{\Theta}\right)^2}{\sum_{p=1}^{N^g}\sum_{q=1}^{N^r} \Re_{p,q}^{\Theta}} \tag{67}$$

VIII.4 run0_length, run45_length, run90_length, run135_length

These features estimate the nonuniformity of the run lengths, taking on their lowest values when the runs are equally distributed throughout the lengths.

$$\text{run}\theta\_\text{length} = \frac{\sum_{q=1}^{N^r}\left(\sum_{p=1}^{N^g} \Re_{p,q}^{\Theta}\right)^2}{\sum_{p=1}^{N^g}\sum_{q=1}^{N^r} \Re_{p,q}^{\Theta}} \tag{68}$$

VIII.5 run0_percent, run45_percent, run90_percent, run135_percent

These features are calculated as the ratio of the total number of possible runs to the object's area, having its lowest value for pictures with the most linear structure.

$$\text{run}\theta\_\text{percent} = \frac{\sum_{p=1}^{N^g}\sum_{q=1}^{N^r}(\Re_{p,q}^{\Theta})}{A} \tag{69}$$

where A is the object's area.

VIII.6 texture_orient

This feature estimates the dominant orientation of the object's linear texture.

$$\text{texture\_orient} = \frac{180}{\pi}\left(\frac{\pi}{2} + arctan\left[\frac{(\lambda_1' - y_{pseudo-moment2})}{xy_{pseudo-cross\_moment2}}\right]\right) \tag{70}$$

where λ_1' is the maximal eigenvalue of the run length pseudo-second moment matrix (calculated in analogy to Section II.9). The run length pseudo-second moments are calculated as follows:

$$x_{pseudo-moment2} = \sum_{p=1}^{N^g}\sum_{q=1}^{N^r}\left[\Re_{p,q}^{0}\sum_{l=1}^{q}(l^2 - l)\right] \tag{71}$$

$$y_{pseudo-moment2} = \sum_{p=1}^{N^g}\sum_{q=1}^{N^r}\left[\Re_{p,q}^{90}\sum_{l=1}^{q}(l^2 - l)\right] \tag{72}$$

$$xypseudo-cross\_moment2 = \frac{\left(\sum_{p=1}^{N^g}\sum_{q=1}^{N^r}\left[\Re_{p,q}^{45}\cdot\sum_{l=1}^{q}(2l^2 - \sqrt{2}l)\right] - \sum_{p=1}^{N^g}\sum_{q=1}^{N^r}\left[\Re_{p,q}^{135}\cdot\sum_{l=1}^{q}(2l^2 - \sqrt{2}l)\right]\right)}{2\sqrt{2}} \tag{73}$$

Orientation is defined as it is for cell_orient, Section II.9, as the angle (measured in a clockwise sense) between the y axis and the dominant orientation of the image's linear structure.

VIII.7 size_txt_orient

This feature amplifies the texture orientation for long runs.

$$\text{size\_txt\_orient} = \frac{\lambda_1'}{\lambda_2'} \tag{74}$$

where λ_1', λ_2' are the maximal and minimal eigenvalues of the run_length pseudo-second moment matrix, defined in Section VIII.6.

Each of the above features are calculated for each in-focus object located in the image. Certain features are used by the classifier to separate artifacts from cell nuclei and to distinguish cells exhibiting MACs from normal cells. As indicated above, it is not possible to predict which features will be used to distinguish artifacts from cells or MAC cells from non-MAC cells, until the classifier has been completely trained and produces a binary decision tree or linear discriminant function.

In the present embodiment of the invention, it has been determined that thirty (30) of the above-described features appear more significant in separating artifacts from genuine nuclei and identifying cells with MACs. These primarily texture features are as follows:

30 preferred nuclear features

1) Area	11) high DNA amount	21) run 90 percent
2) mean radius	12) high average distance	22) run 135 percent
3) OD variance	13) mid/high average distance	23) grey level 0
4) OD skewness	14) correlation	24) grey level 45
5) range average	15) homogeneity	25) grey level 90
6) OD maximum	16) entropy	25) grey level 135
7) density of light spots	17) fractal dimension	27) run length 0
8) low DNA area	18) DNA index	28) run length 45
9) high DNA area	19) run 0 percent	29) run length 90
10) low DNA amount	20) run 45 percent	30) run length 135

Although these features have been found to have the best ability to differentiate between types of cells, other object types may be differentiated by the other features described above.

As indicated above, the ability of the system according to the present invention to distinguish cell nuclei from artifacts or cells that exhibit MACs from those that do not depends on the ability of the classifier to make distinctions based on the values of the features computed. For example, to separate cell nuclei from artifacts, the present

invention may apply several different discriminant functions each of which is trained to identify particular types of objects. For example, the following discriminant function has been used in the presently preferred embodiment of the invention to separate intermediate cervical cells from small picnotic objects:

	cervical cells	**picnotic**
max_radius	4.56914	3.92899
freq_low_fft	-.03624	-.04714
harmon03_fft	1.29958	1.80412
harmon04.fft	.85959	1.20653
lowVSmed_DNA	58.83394	61.84034
energy	6566.14355	6182.17139
correlation	.56801	.52911
homogeneity	-920.05017	-883.31567
cl_shade	-67.37746	-63.68423
den_drk_spot	916.69360	870.75739
CONSTANT	-292.92908	-269.42419

Another discriminant function that can separate cells from junk particles is:

	cells	**junk**
eccentricity	606.67365	574.82507
compactness	988.57196	1013.19745
freq_low_fft	-2.57094	-2.51594
freq_high_fft	-28.93165	-28.48727
harmon02.fft	-31.30210	-30.18383
harmon03.fft	14.40738	14.30784
medDNAamnt	39.28350	37.50647
correlation	.27381	.29397
CONSTANT	-834.57800	-836.19659

Yet a third discriminant function that can separate folded cells that should be ignored from suitable cells for analysis.

	normal interm	**rejected objects**
sphericity	709.66357	701.85864
eccentricity	456.09146	444.18469
compactness	1221.73840	1232.27441
elongation	-391.76352	-387.19376

freq_high_fft	-37.89624	-37.39510
lowDNAamnt	-41.89951	-39.42714
low_den_obj	1.40092	1.60374
correlation	.26310	.29536
range_average	.06601	.06029
CONSTANT	-968.73628	-971.18219

Obviously, the particular linear discriminant function produced by the classifier will depend on the type of classifier used and the training sets of cells. The above examples are given merely for purposes of illustration.

As can be seen, the present invention is a system that automatically detects malignancy-associated changes in a cell sample. By properly staining and imaging a cell sample, the features of each object found on the slide can be determined and used to provide an indication whether the patient from which the cell sample was obtained is normal or abnormal. In addition, MACs provide an indication of whether cancer treatment given is effective as well as if a cancer is in remission.

While the preferred embodiment of the invention has been illustrated and described, it will be appreciated that various changes can be made therein without departing from the spirit and scope of the invention.

The embodiments of the invention in which an exclusive property or privilege is claimed are defined as follows:

1. A method of detecting malignancy-associated changes in a cell sample, comprising the steps of:

obtaining a cell sample;

staining the sample to identify cell nuclei within the sample;

obtaining an image of the cell sample with a digital microscope of the type that includes a digital CCD camera and a programmable slide stage;

focusing the image;

identifying objects in the image;

calculating a set of feature values for each object; and

analyzing the feature values to determine whether each object is a cell nucleus having malignancy-associated changes.

2. The method of Claim 1, wherein each object in the cell image comprises a group of pixels each of which has an intensity value, wherein the step of identifying objects in the image further comprises the steps of:

computing a histogram of all pixels in the image;

determining an average intensity of background pixels in the image;

determining an average intensity of the object pixels in the image;

determining a threshold that lies between the average intensity of the background pixels and the average intensity of the object pixels; and

identifying every pixel with an intensity greater than the threshold as background and every pixel with an intensity less than or equal to the threshold as an object.

3. The method of Claim 1, wherein each of the objects has an edge that separates the object from the background and wherein the step of identifying objects in the cell image further comprises the steps of:

identifying an edge of the object by performing the steps of:

creating an annular ring that surrounds the object by dilating the edge of the object to define an outer edge of the annular ring and eroding the edge of the object to define an inner edge of the annular ring;

calculating a gradient value of each pixel in the annular ring; and

removing pixels from the annular ring having lower gradients until the annular ring comprises a single pixel chain that encircles the object.

4. The method of Claim 3, wherein the step of calculating one or more features of the set of feature values further comprises the step of:

dilating or contracting the true edge of the object before calculating the features.

5. The method of Claim 1, wherein the image is stored in a memory of a computer system, the method further comprising the steps of:

adjusting the local focus of each object by obtaining a series of images at different stage positions;

for each object, selecting the image where the focus of the object is best; and

overwriting the memory of the computer with the image of each object at its best focus.

6. The method of Claim 5, further comprising the step of:

compensating the image for variations in illumination intensity of a light source of the digital microscope by:

reading a test image obtained from a blank slide in the digital microscope;

subtracting the intensity value of each pixel of the test image from a corresponding pixel in the image of the cell sample;

determining the average intensity of the pixels in the test image; and

adding the average intensity to each pixel of the image obtained from the cell sample.

7. The method of Claim 6, further comprising the step of compensating for local absorbency around the object by:

determining an average pixel intensity for a group of pixels near the object; and

subtracting the average pixel intensity for the group of pixels near the object from each pixel that is included in the object.

8. The method of Claim 7, wherein the group of pixels near the object are defined by a square boundary having an area slightly greater than an area of the object.

9. The method of Claim 1, further comprising the steps of:

removing artifacts from the image by calculating the area, shape and optical density for each object; and

removing from the image any object with an area > 2,000 square microns, any objects with a shape or sphericity greater than 4 and an optical density greater than 1c.

10. The method of Claim 1, wherein the features used to separate cell nuclei having malignancy-associated changes from nuclei not having malignancy-associated changes are selected from the group comprising:

1) Area	11) high DNA amount	21) run 90 percent
2) mean radius	12) high average distance	22) run 135 percent
3) OD variance	13) mid/high average distance	23) grey level 0
4) OD skewness	14) correlation	24) grey level 45
5) range average	15) homogeneity	25) grey level 90
6) OD maximum	16) entropy	25) grey level 135
7) density of light spots	17) fractal dimension	27) run length 0
8) low DNA area	18) DNA index	28) run length 45
9) high DNA area	19) run 0 percent	29) run length 90
10) low DNA amount	20) run 45 percent	30) run length 135

11. A method of predicting whether a patient will develop cancer, comprising the steps of:

obtaining a sample of apparently normal cells from the patient;

determining whether the cells in the sample exhibit malignancy associated changes by:

(1) staining the nuclei of the cells in the sample;

(2) obtaining an image of the cells with a digital microscope and recording the image in a computer system;

(3) analyzing the stored image of the cells to identify the nuclei;

(4) computing a set of feature values for each nucleus found in the sample and from the feature values determining whether the nucleus exhibits a malignancy associated change; and

determining a total number of nuclei in the sample that exhibit malignancy-associated changes and from the number predicting whether the patient will develop cancer.

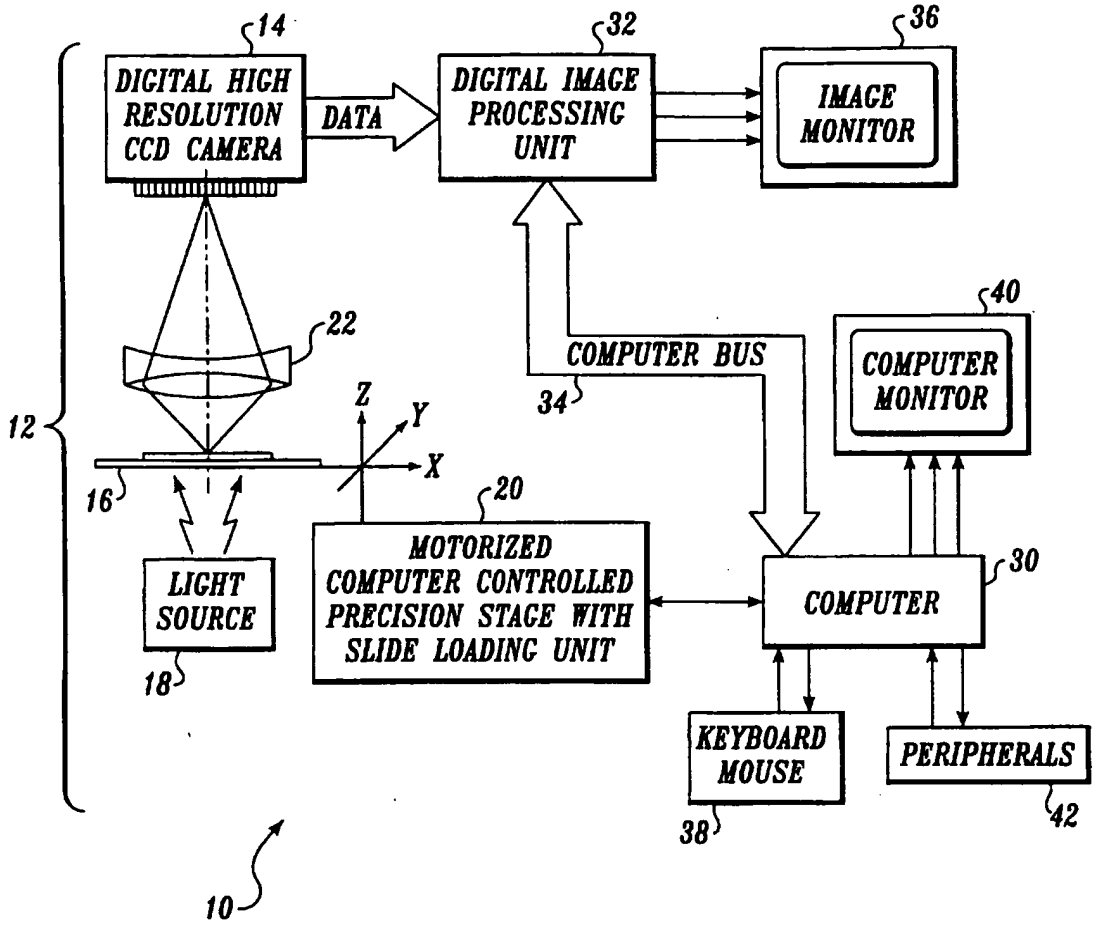

Fig. 1

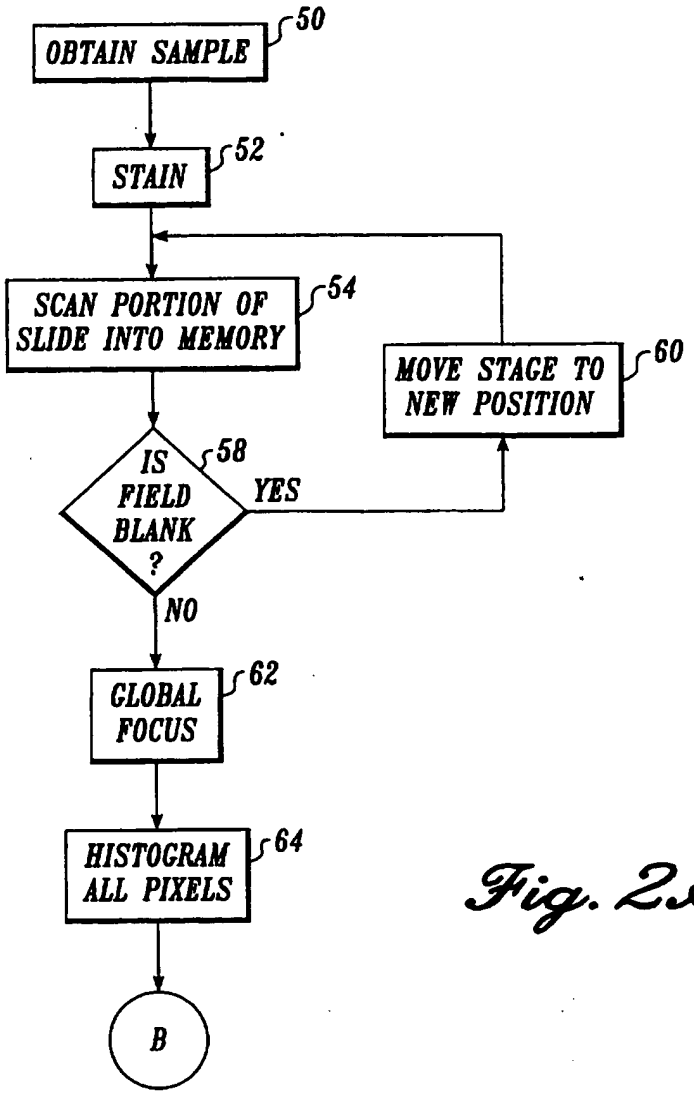

Fig. 2A

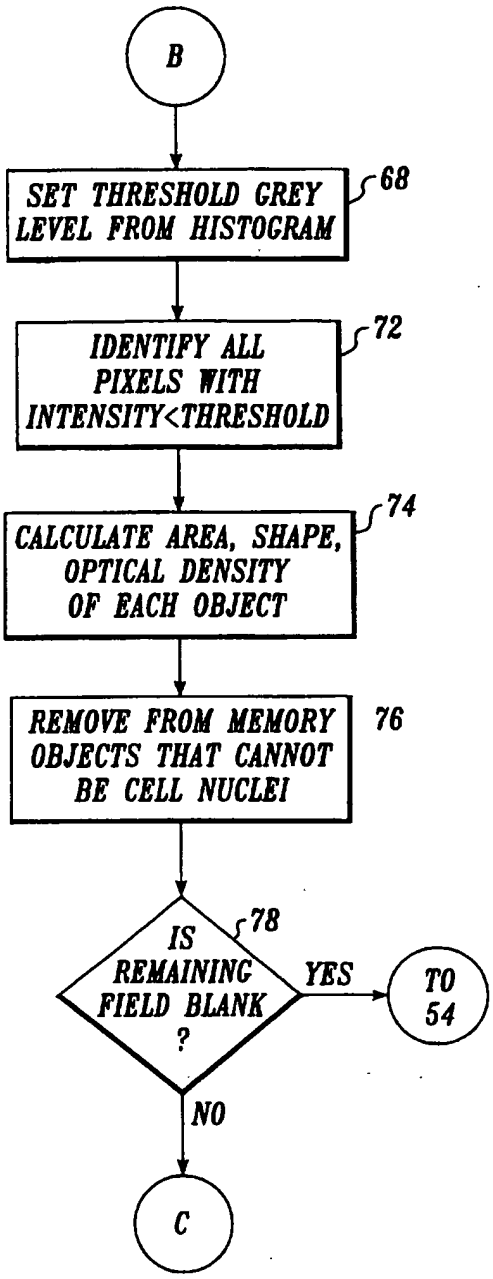

Fig. 2B

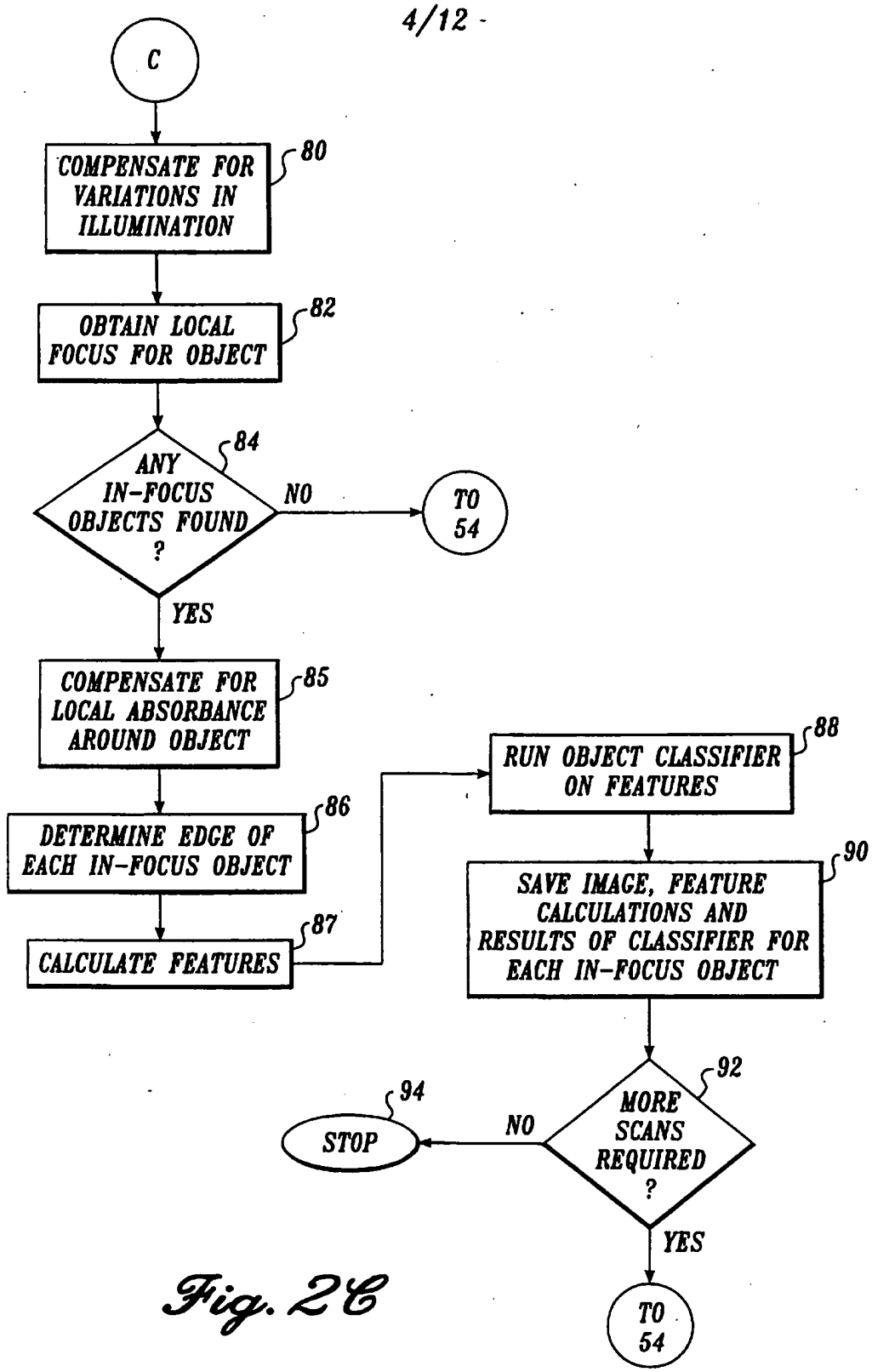

Fig. 2C

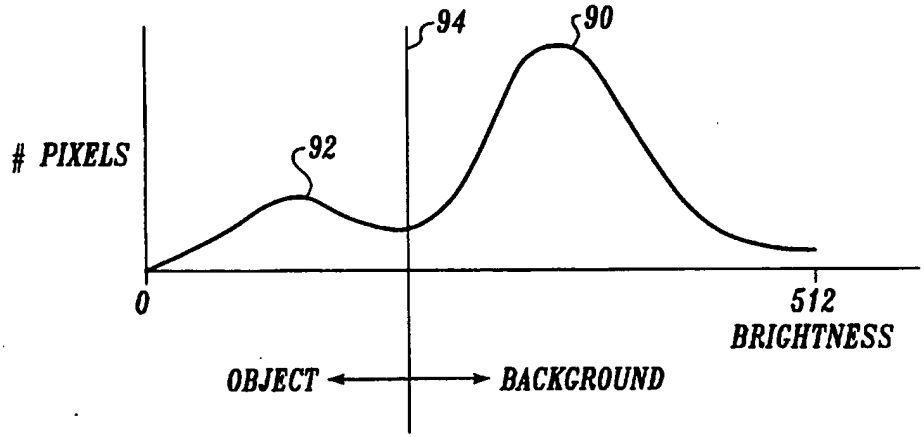

Fig. 3

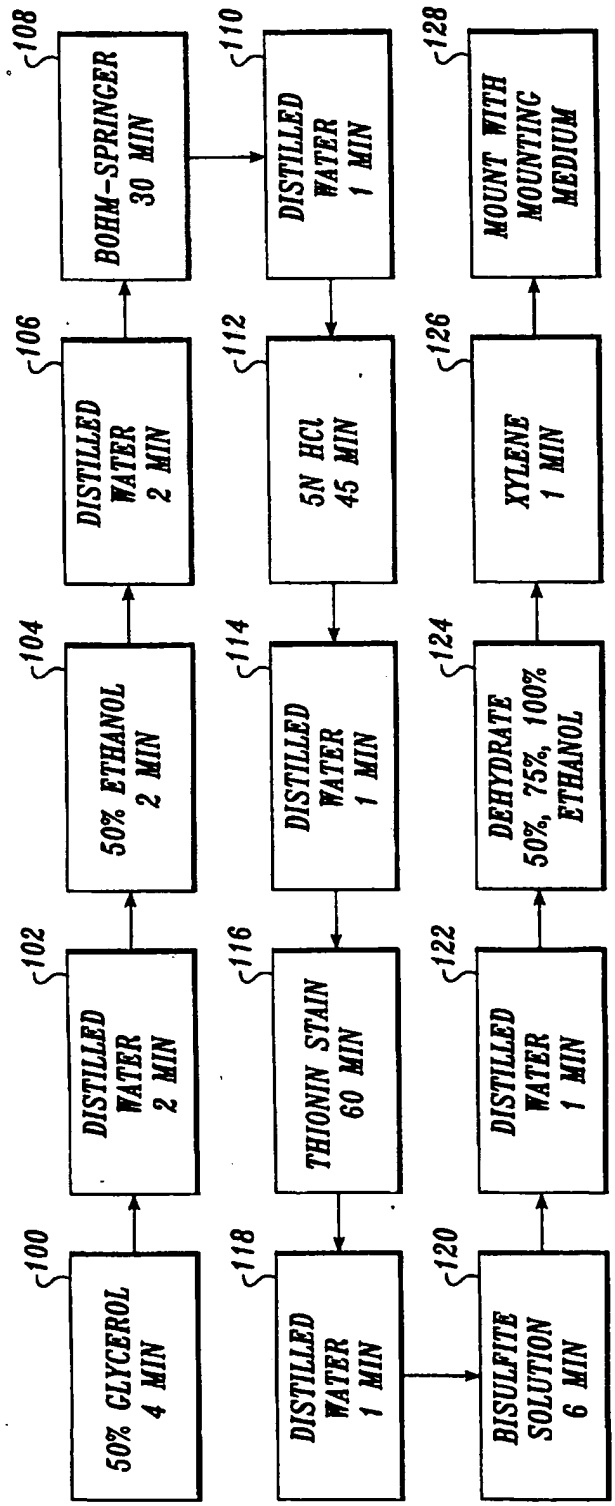

Fig. 4

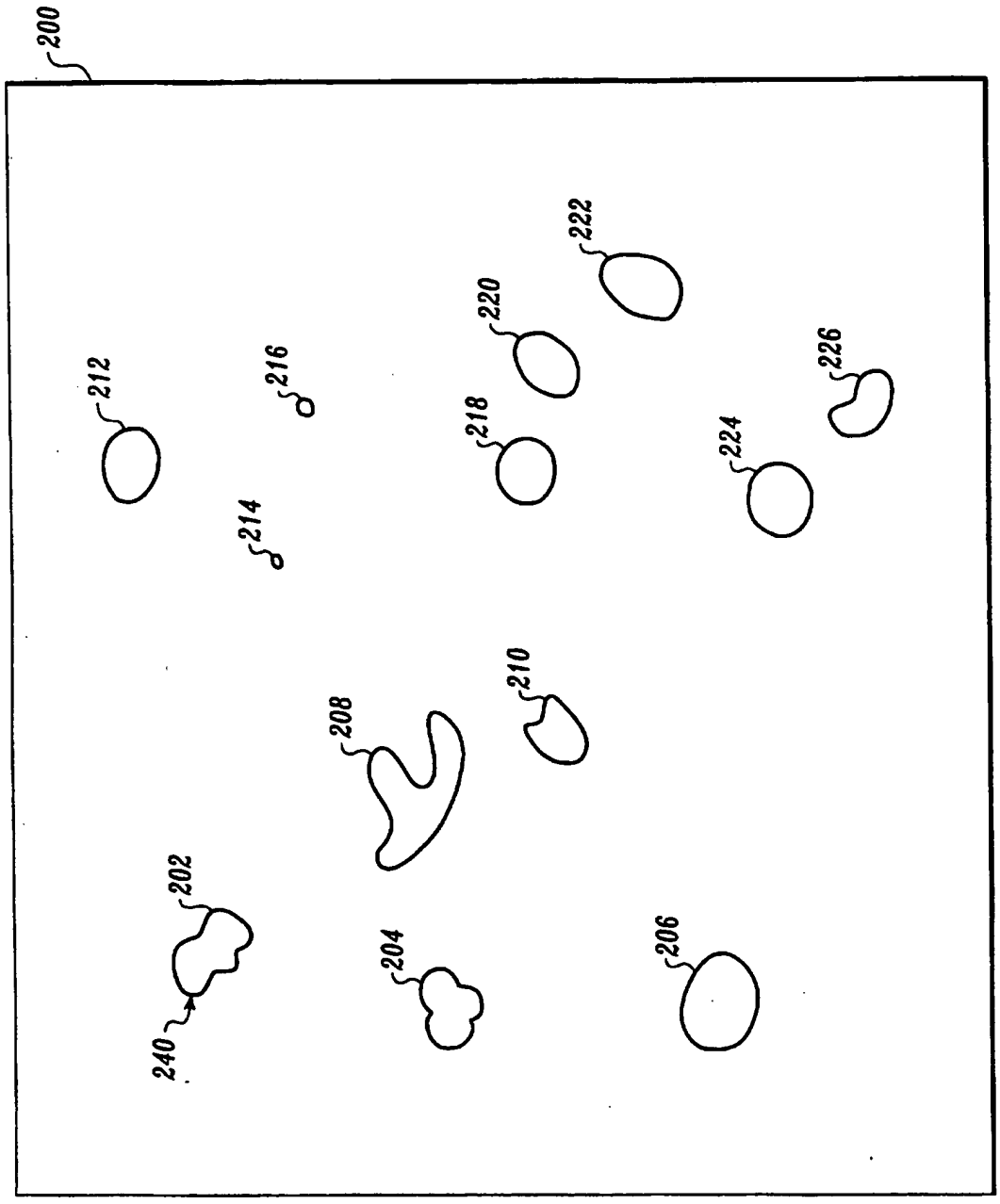

Fig. 5

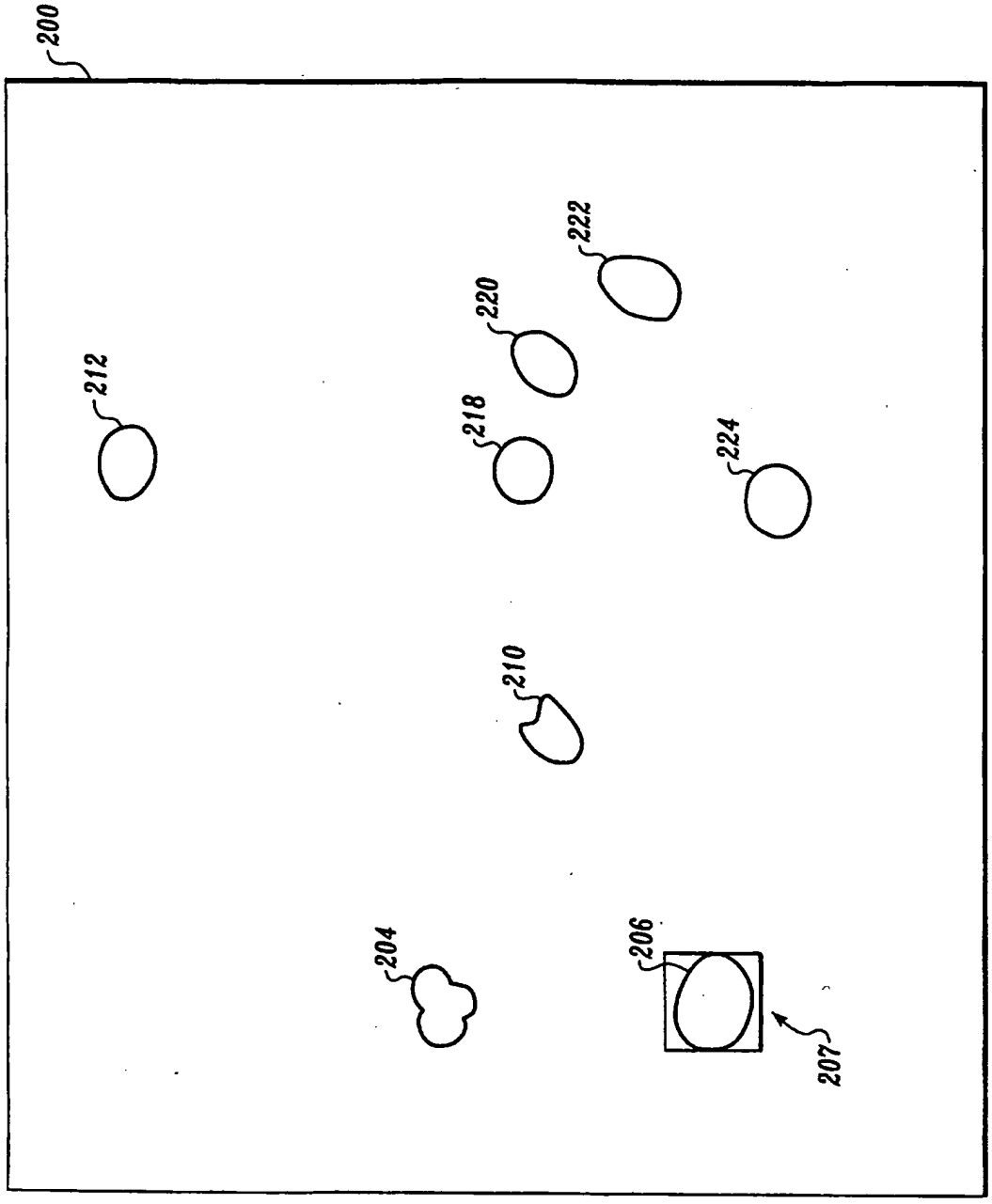

Fig. 6

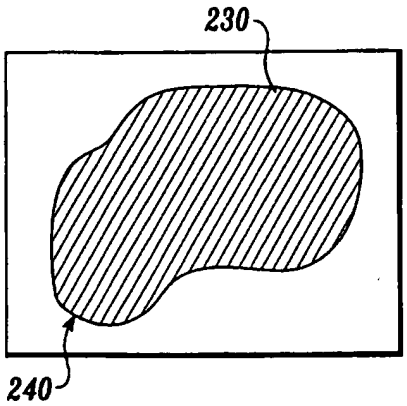

Fig. 7A

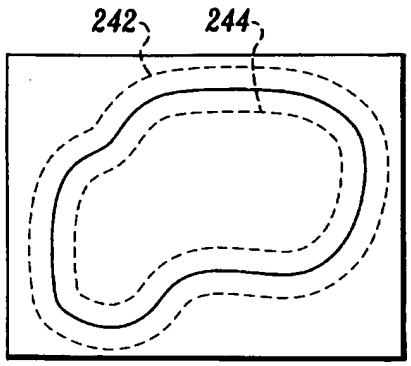

Fig. 7B

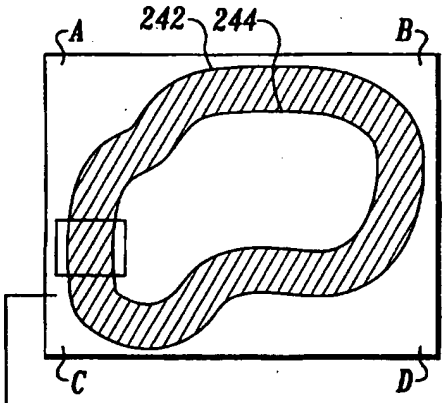

Fig. 7C

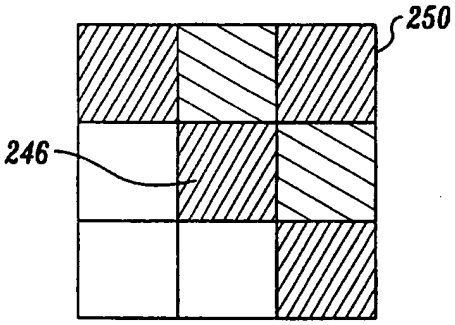

Fig. 7E

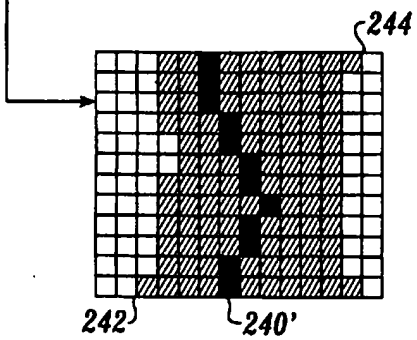

Fig. 7D

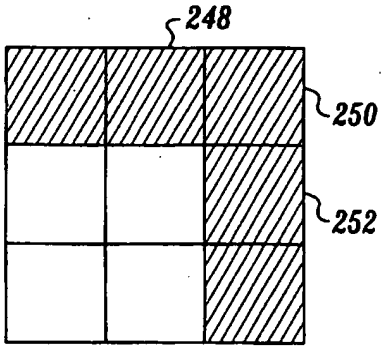

Fig. 7F

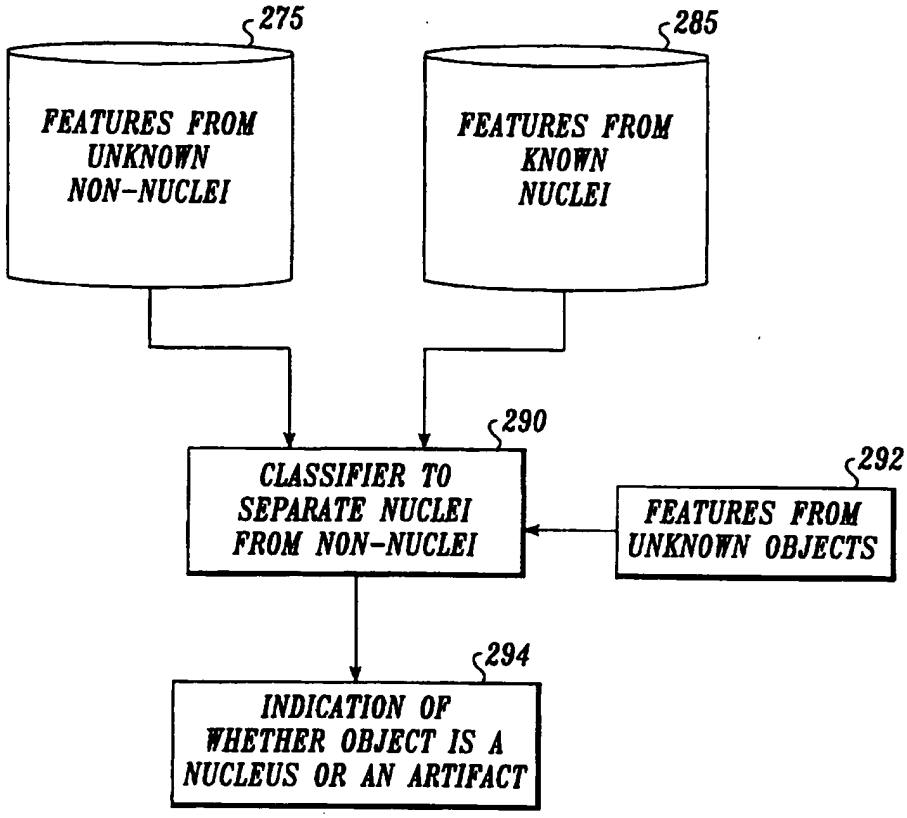

Fig. 8

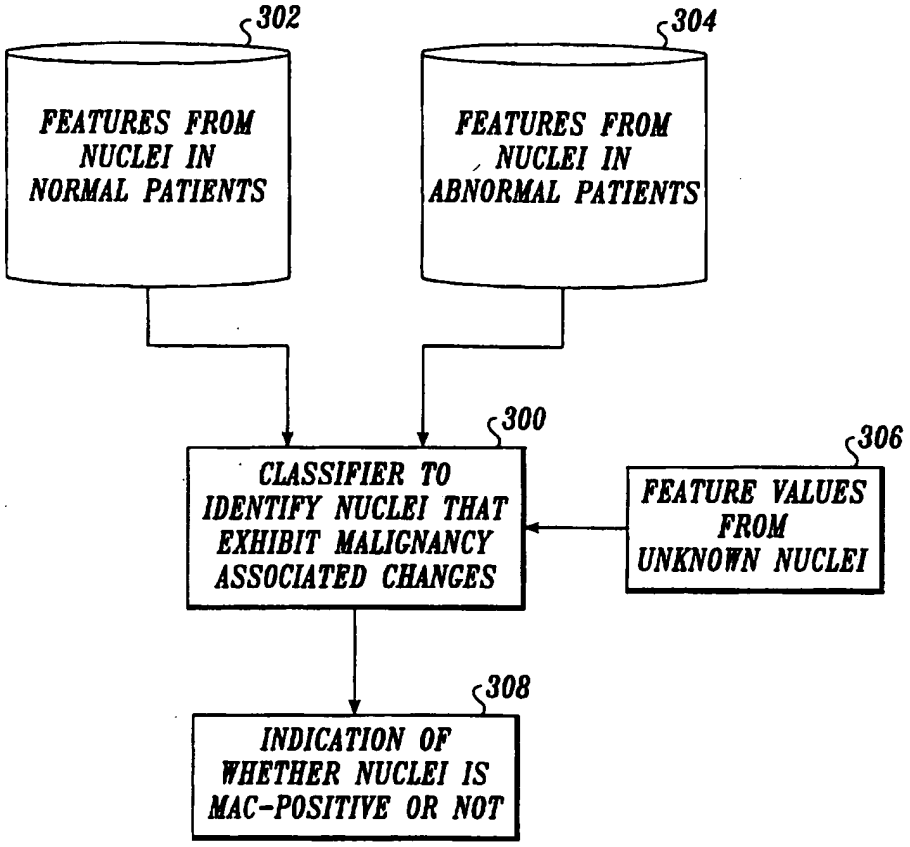

Fig. 9

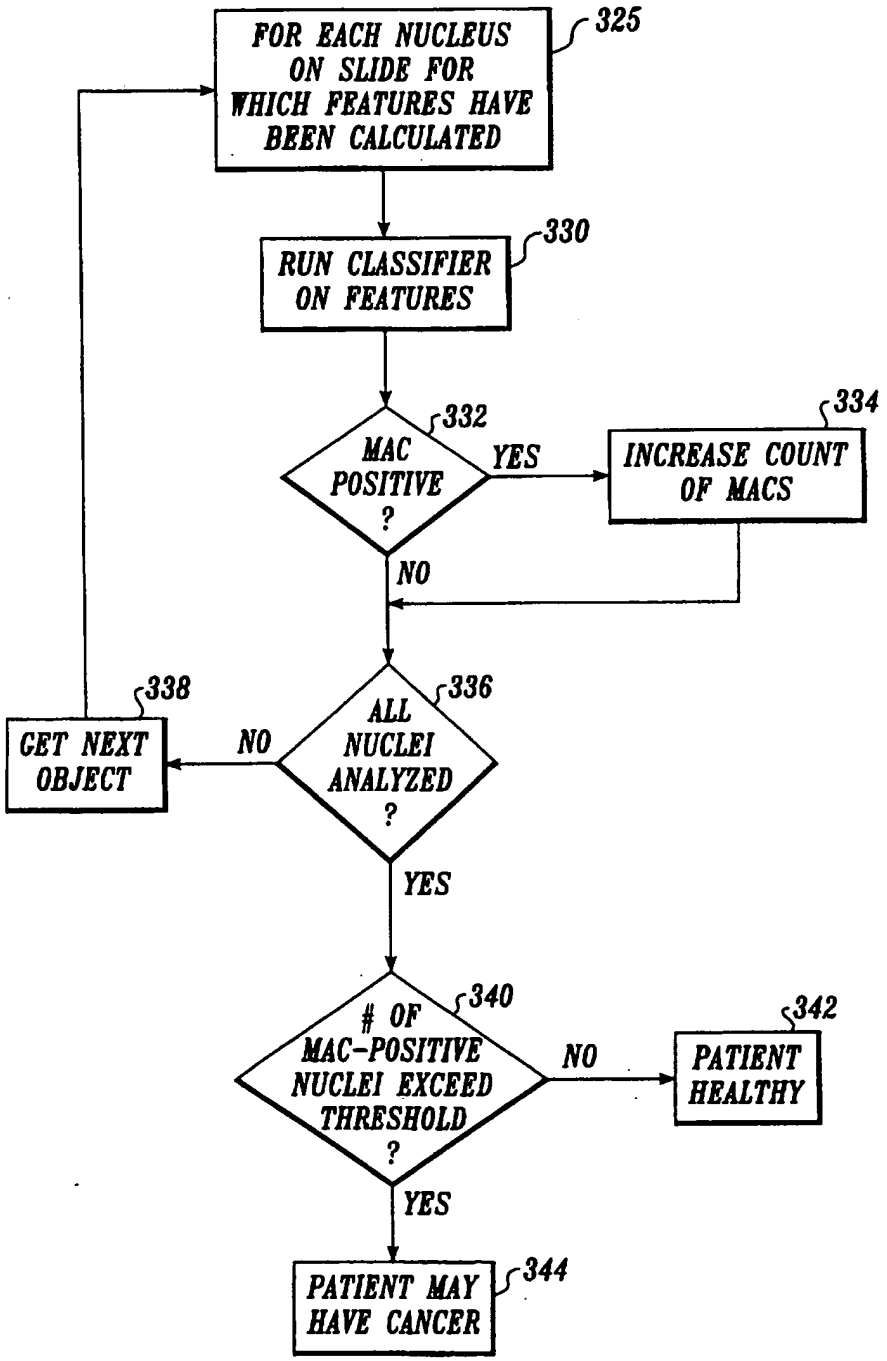

Fig. 10

INTERNATIONAL SEARCH REPORT

Inte ...nal Application No
PCT/CA 97/00301

A. CLASSIFICATION OF SUBJECT MATTER
IPC 6 G06K9/00 G01N15/14

According to International Patent Classification (IPC) or to both national classification and IPC

B. FIELDS SEARCHED

Minimum documentation searched (classification system followed by classification symbols)
IPC 6 G06K G01N G06T

Documentation searched other than minimum documentation to the extent that such documents are included in the fields searched

Electronic data base consulted during the international search (name of data base and, where practical, search terms used)

C. DOCUMENTS CONSIDERED TO BE RELEVANT

Category *	Citation of document, with indication, where appropriate, of the relevant passages	Relevant to claim No.
X	WO 96 09594 A (NEOPATH INC) 28 March 1996 see page 1 - page 14; claim 21	1,11
X	WO 96 09605 A (NEOPATH INC) 28 March 1996 see page 1 - page 11	1,11
Y	EP 0 595 506 A (XILLIX TECHNOLOGIES CORP) 4 May 1994 cited in the application see the whole document	1,2,11
Y	WO 93 16442 A (NEOPATH INC) 19 August 1993 see page 1 - page 9, line 25; figure 4A	1,2,11

-/--

[X] Further documents are listed in the continuation of box C.

[X] Patent family members are listed in annex.

* Special categories of cited documents :

"A" document defining the general state of the art which is not considered to be of particular relevance

"E" earlier document but published on or after the international filing date

"L" document which may throw doubts on priority claim(s) or which is cited to establish the publication date of another citation or other special reason (as specified)

"O" document referring to an oral disclosure, use, exhibition or other means

"P" document published prior to the international filing date but later than the priority date claimed

"T" later document published after the international filing date or priority date and not in conflict with the application but cited to understand the principle or theory underlying the invention

"X" document of particular relevance; the claimed invention cannot be considered novel or cannot be considered to involve an inventive step when the document is taken alone

"Y" document of particular relevance; the claimed invention cannot be considered to involve an inventive step when the document is combined with one or more other such documents, such combination being obvious to a person skilled in the art.

"&" document member of the same patent family

Date of the actual completion of the international search	Date of mailing of the international search report
23 July 1997	- 6. 08. 97

Name and mailing address of the ISA	Authorized officer
European Patent Office, P.B. 5818 Patentlaan 2 NL - 2280 HV Rijswijk Tel. (+ 31-70) 340-2040, Tx. 31 651 epo nl, Fax: (+ 31-70) 340-3016	Brison, O

Form PCT/ISA/210 (second sheet) (July 1992)

INTERNATIONAL SEARCH REPORT

Int. ional Application No
PCT/CA 97/00301

C.(Continuation) DOCUMENTS CONSIDERED TO BE RELEVANT

Category *	Citation of document, with indication, where appropriate, of the relevant passages	Relevant to claim No.
Y	TRAC, TRENDS IN ANALYTICAL CHEMISTRY, vol. 10, no. 8, 1 September 1991, AMSTERDAM, NL, pages 237-243, XP000219625 BERTRAND D ET AL: "BASICS OF VIDEO IMAGE ANALYSIS" see page 239 - page 240 ---	2
A	EP 0 610 916 A (CEDARS SINAI MEDICAL CENTER) 17 August 1994 see the whole document ---	1,3,11
X	WO 93 16436 A (NEOPATH INC) 19 August 1993 see claims 1,2 ---	1,11
A	WO 90 10277 A (CELL ANALYSIS SYSTEMS INC) 7 September 1990 see page 11 - page 14, line 30 ---	1,2,11
A	WO 91 15826 A (NEUROMEDICAL SYSTEMS INC) 17 October 1991 see page 6, line 15 - page 10, line 26 -----	1,5,11

Form PCT/ISA/210 (continuation of second sheet) (July 1992)

INTERNATIONAL SEARCH REPORT

Information on patent family members

Inte nal Application No
PCT/CA 97/00301

Patent document cited in search report	Publication date	Patent family member(s)	Publication date
WO 9609594 A	28-03-96	AU 3629295 A	09-04-96
WO 9609605 A	28-03-96	AU 3629795 A	09-04-96
EP 0595506 A	04-05-94	CA 2086785 A	15-04-94
		JP 6231229 A	19-08-94
WO 9316442 A	19-08-93	AU 671984 B	19-09-96
		AU 3737693 A	03-09-93
		AU 7545096 A	20-02-97
		CA 2130340 A	19-08-93
		EP 0664038 A	26-07-95
		JP 7504056 T	27-04-95
		US 5528703 A	18-06-96
EP 0610916 A	17-08-94	NONE	
WO 9316436 A	19-08-93	AU 670938 B	08-08-96
		AU 3722893 A	03-09-93
		CA 2130338 A	19-08-93
		EP 0628186 A	14-12-94
		JP 7504283 T	11-05-95
WO 9010277 A	07-09-90	CA 2045614 A	25-08-90
		EP 0460071 A	11-12-91
WO 9115826 A	17-10-91	AU 7668191 A	30-10-91
		CA 2064571 A	01-10-91
		EP 0479977 A	15-04-92
		US 5544650 A	13-08-96